Wild Life in the Flow Zoo on a Gas Turbine Blade

Roddam Narasimha
Jawarahlal Nehru Centre for Advanced Scientific Research

(with: S M Deshpande, R Ranjan, N H Maruthi, K S Patel)

20 January 2018
Discussion Meeting on
Turbulence from Angstroms to Light Years
International Centre for Theoretical Sciences

MILD

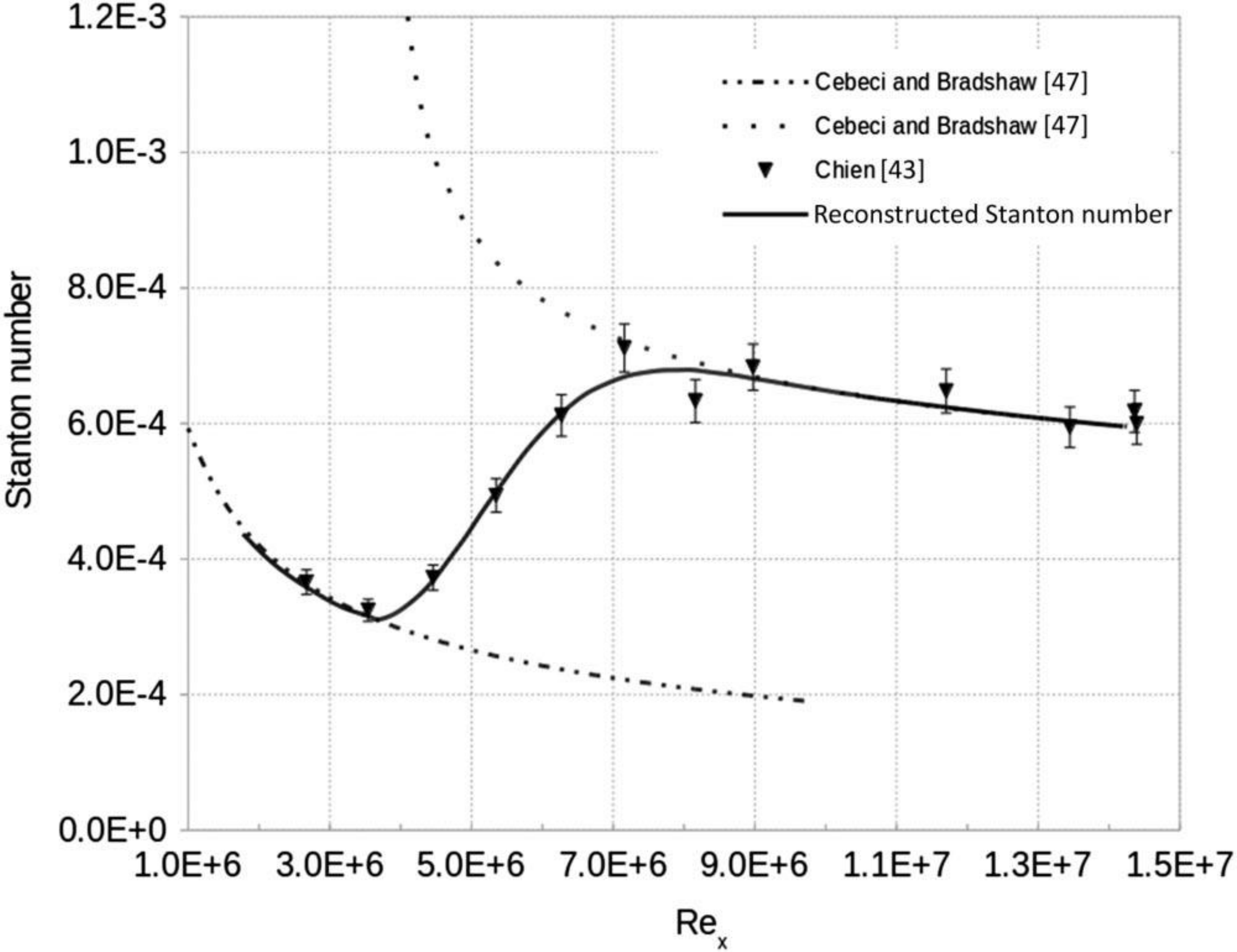

Wall heat transfer on a 5^0 cone during transition from laminar to turbulent at Mach 8. (Chien 1974)

WILD

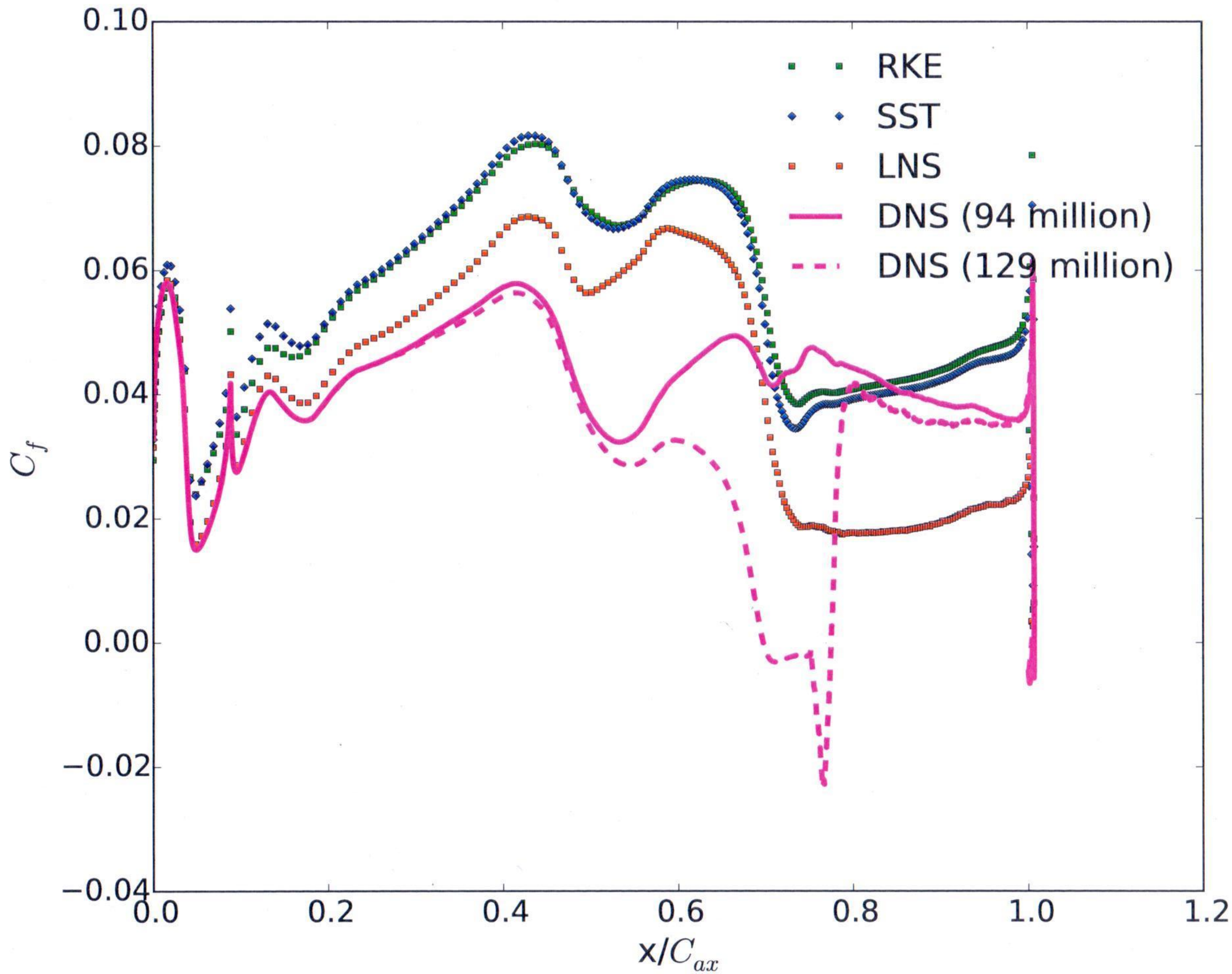

Skin friction coefficient on the suction side on a turbine blade

TURBULENCE RESEARCH

Three 'philosophies'

- Deep science : focus on 'simplest' problem (for example homogeneous isotropic turbulence)

- Technological need : largely RANS, LES, Test Data ('We don't wait to understand the digestive process before eating')

- Dynamics of turbulent shear flows : amazing diversity, rich in ideas, applications, controversies; universe full of crazy, beautiful or fearsome flows

- Major shear flow phenomena (not amenable to RANS)

  (i) Flow separation in wall bounded flows
  (ii) Transition from laminar to turbulent flow
  (iii) Reverse transition from turbulent to laminar / quasi-laminar flow
  (iv) Coherent structures : order in fully turbulent flows
  (v) Effects of curvature, rotation, stratification, heating . . .

THE AMAZING DIVERSITY OF FLUID FLOWS !

That we have written an equation does not remove from the flow of fluids its charm or mystery or its surprise. If such variety is possible in a simple equation with only one parameter, how much more is possible with complex equations !

– Feynman Lectures (1964) II: 41-11

From the point of view of theoretical physics, turbulence is the first clear-cut instance calling for a new form of statistical mechanics. . . .The impact of an adequate theory of turbulence on certain very important parts of pure mathematics may be even greater.

– J von Neumann 1949

CUMULUS CLOUDS

Cumulus congestus

Cumulo nimbus on a Bangalore lake (from Vybhav)

CASCADING WATER

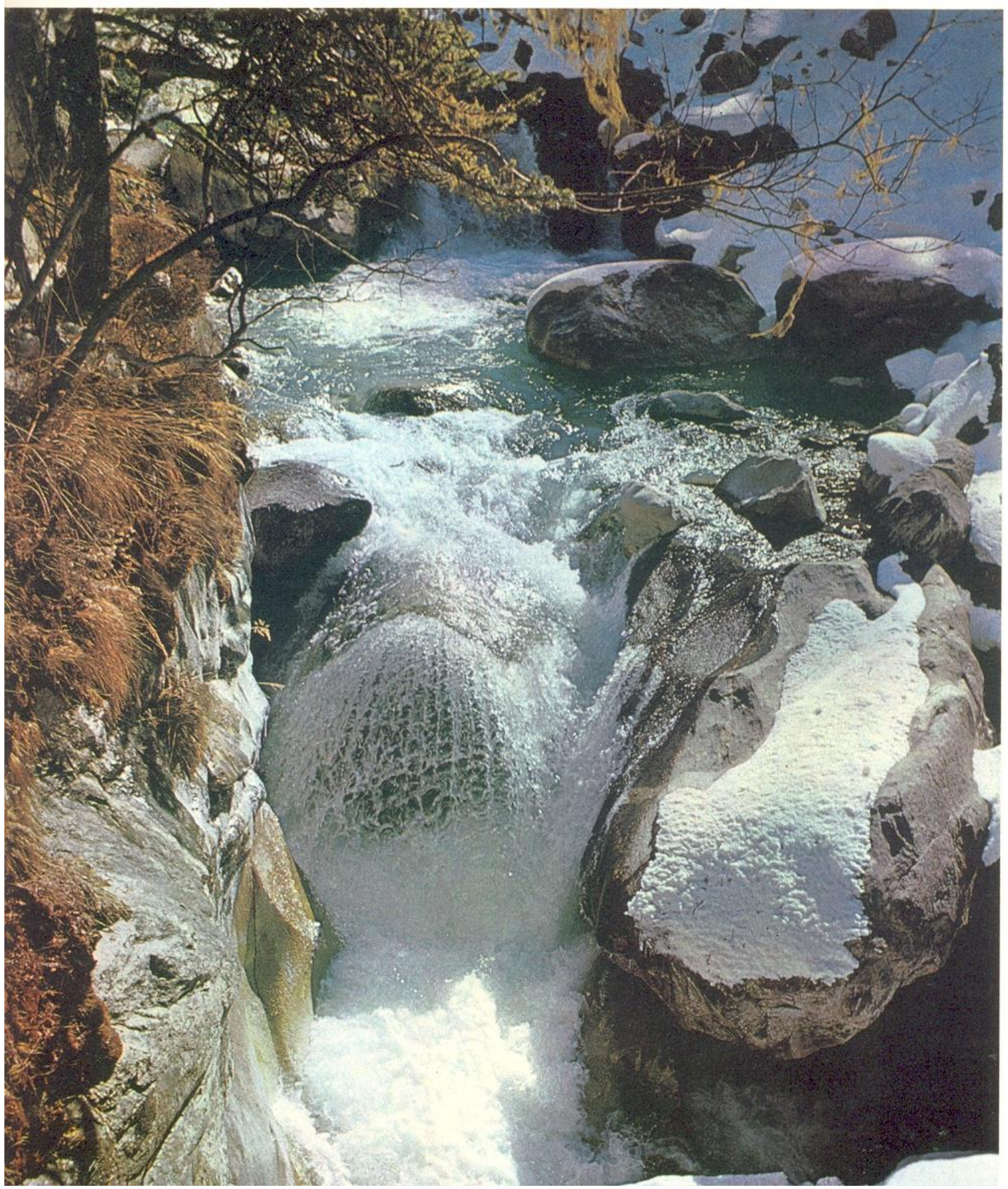

Patterns (middle of the photograph) as water cascades over smooth rock Imja Khola, on way to Mt. Everest (Brower 1966)

AWESOME GRACE

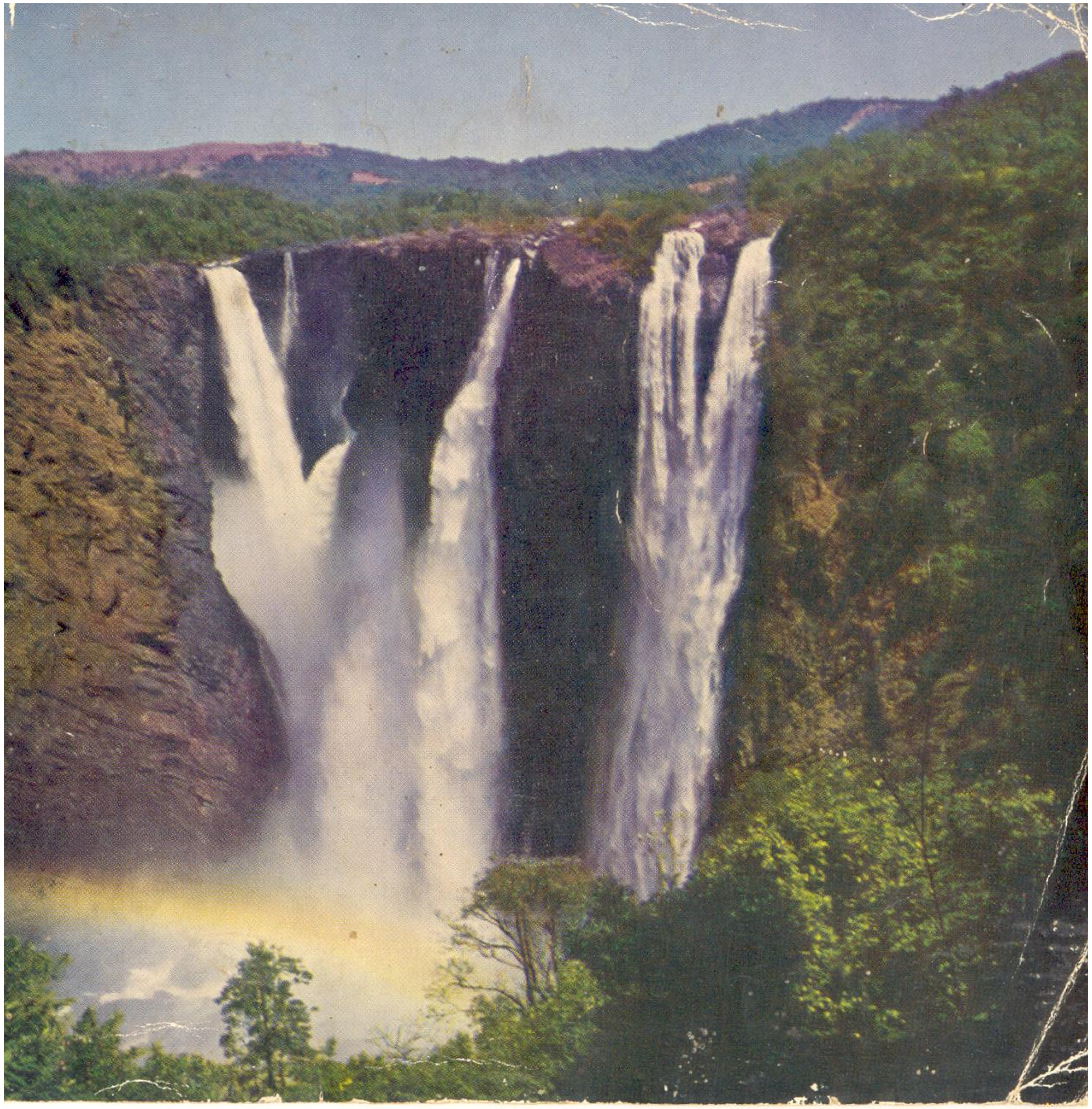

The four waterfalls in Jog, Karnataka. Popularly called Raja, Rocket, Roarer, Rani, they are water flows that are at once majestic, awesome, graceful

TIDAL BORE

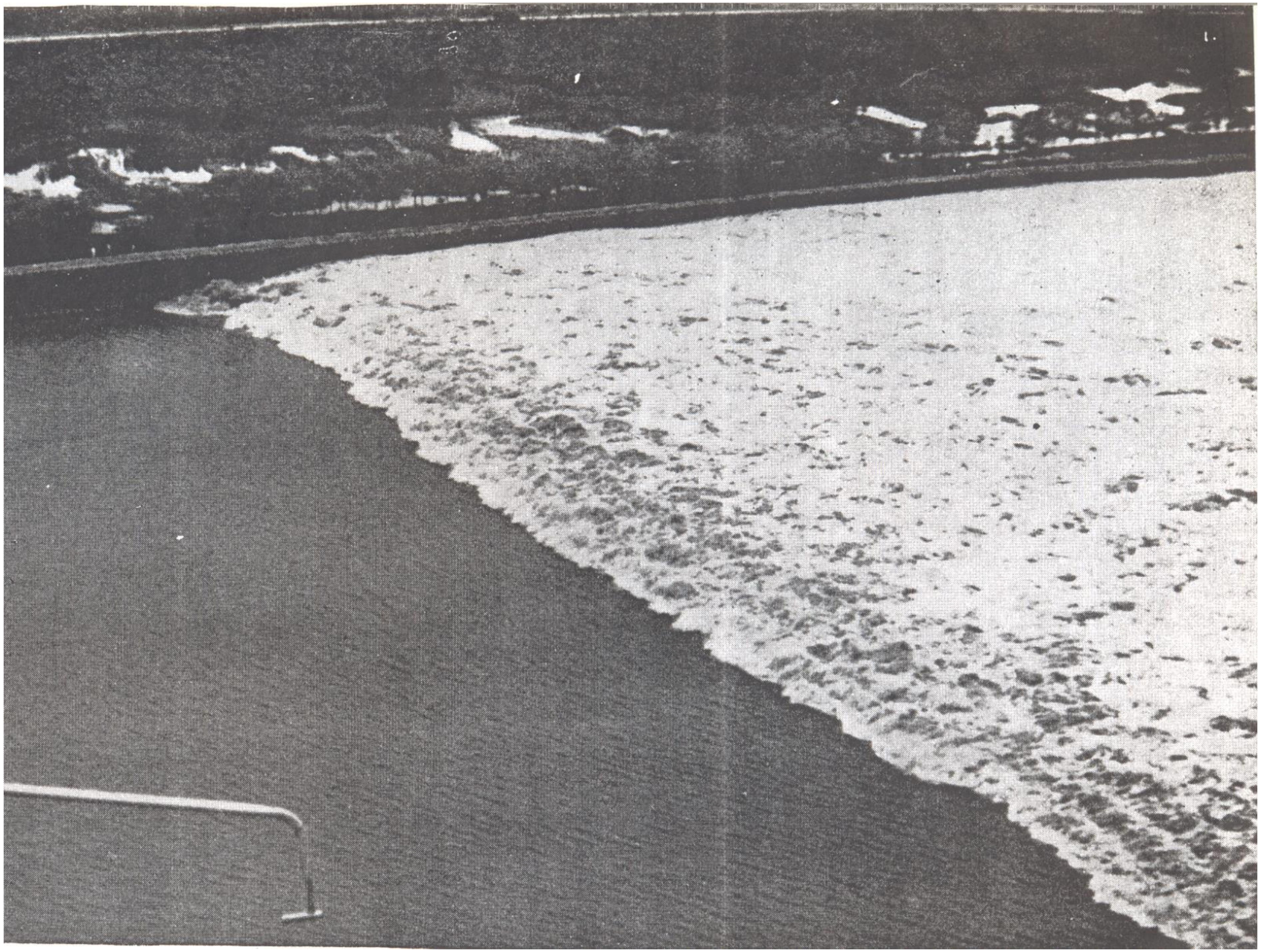

Bore on the river Tsientang, near Hangzhou (= Hanchow), < 200 km SW along coast from Shanghai

A TORNADO

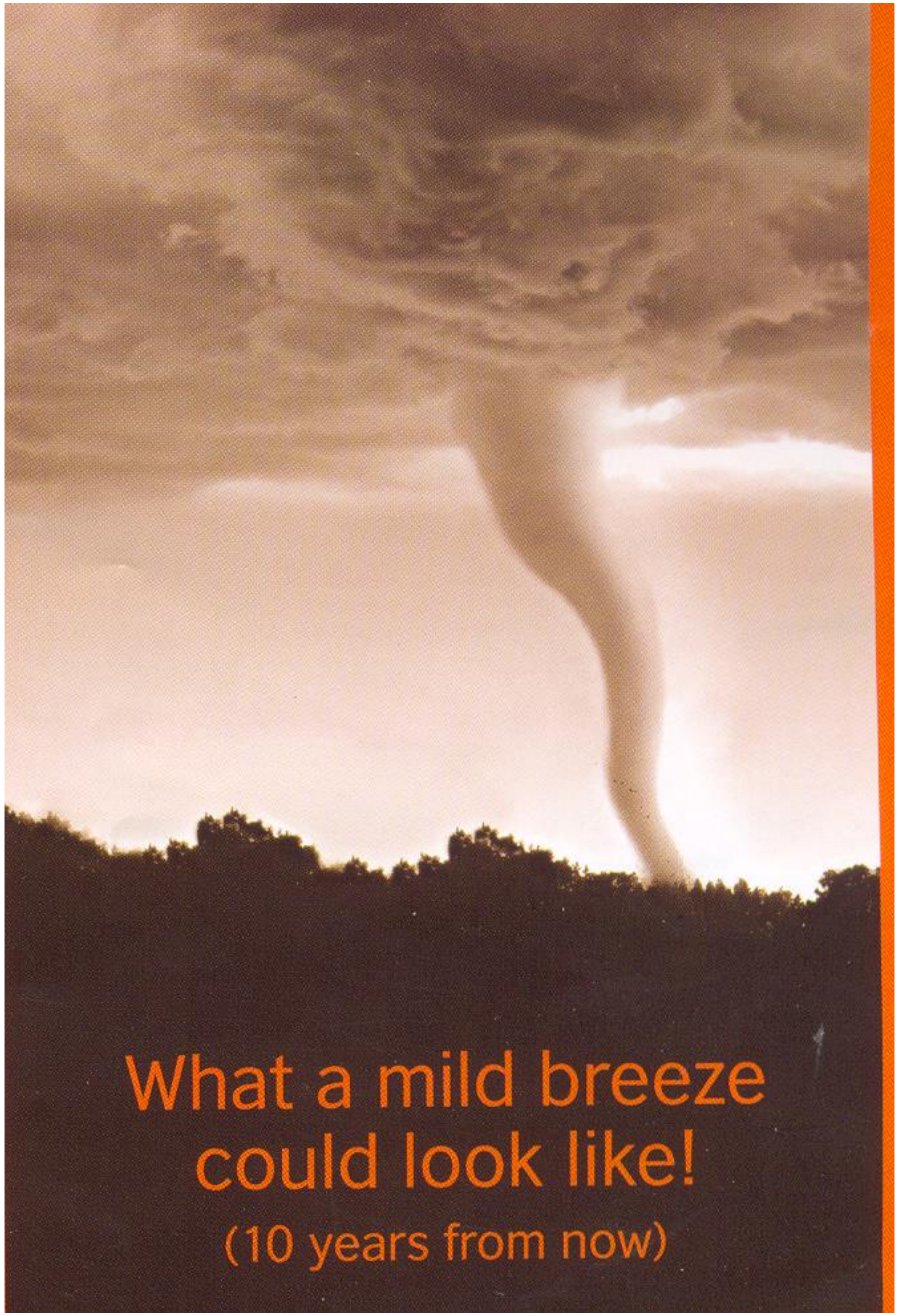

. . . away from the business end

ORDER AND CHAOS OVER E.CHINA SEA

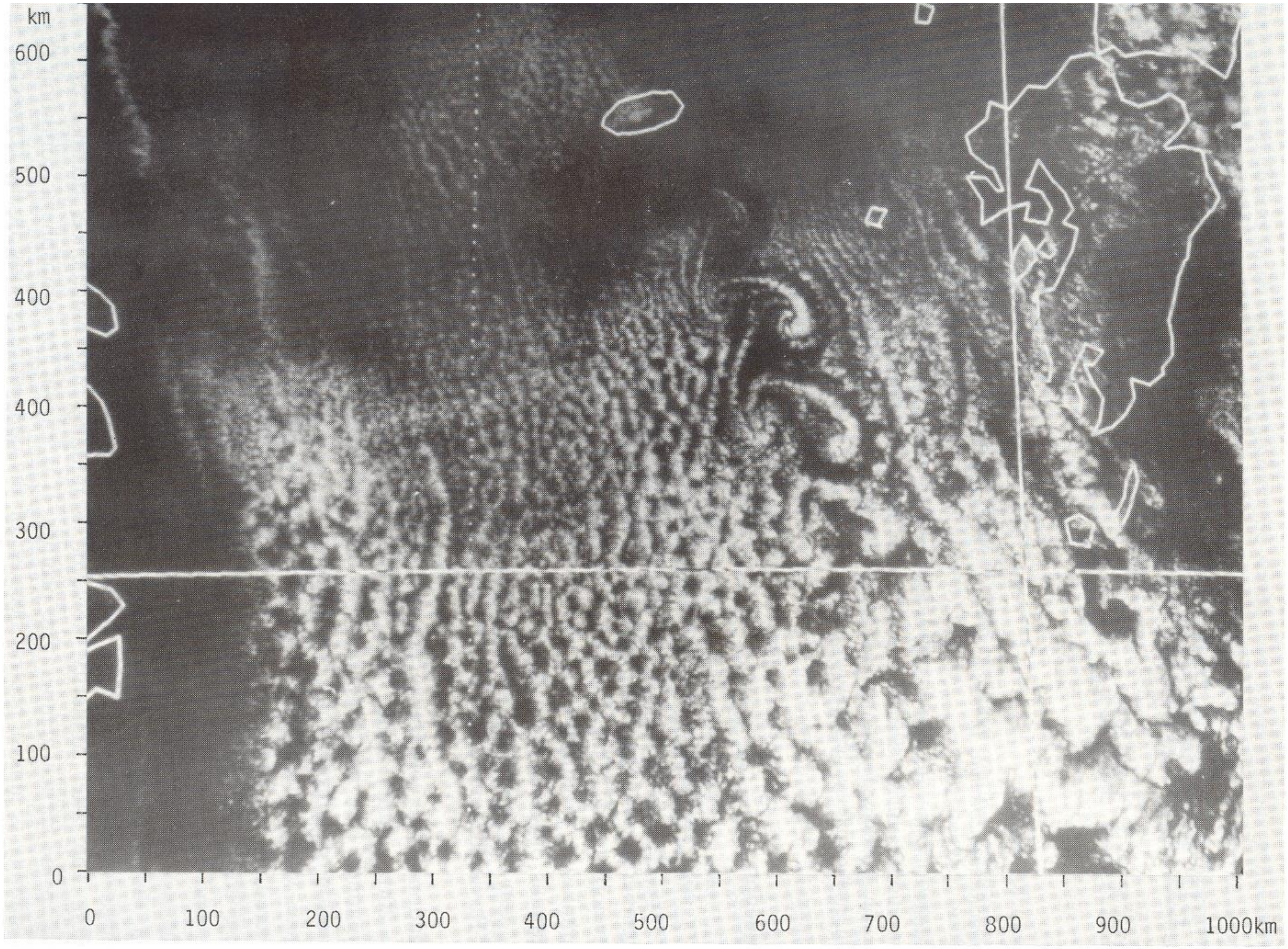

Visible image of GMS (03Z, 4 Dec.1983) in an outbreak of a cold air mass over the warm ocean.

HIGH WAVE NO VORTEX STRUCTURES: HOMOGENEOUS ISOTROPIC TURBULENCE

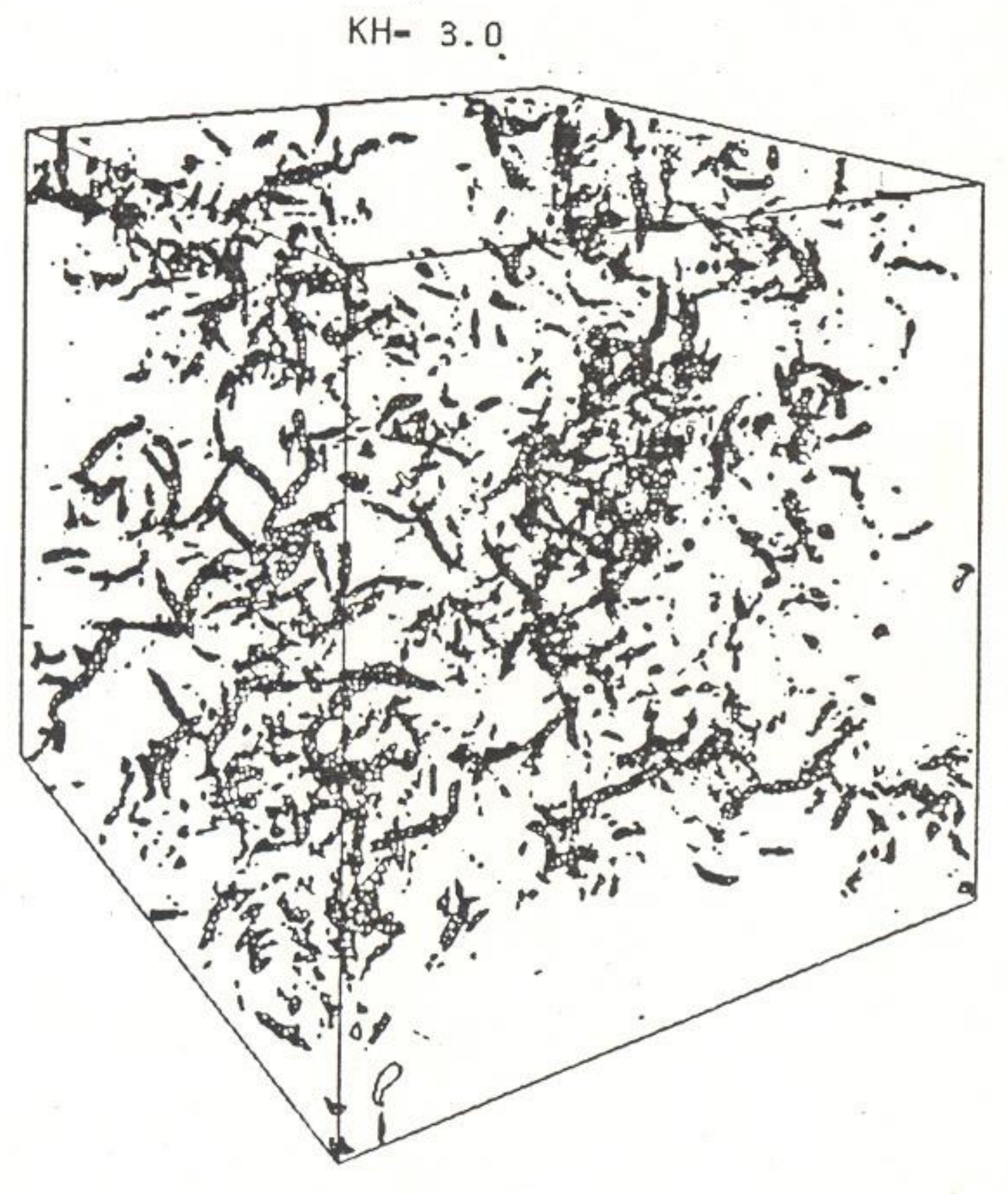

Numerical simulation

GRID TURBULENCE : FLOW VISUALIZATION

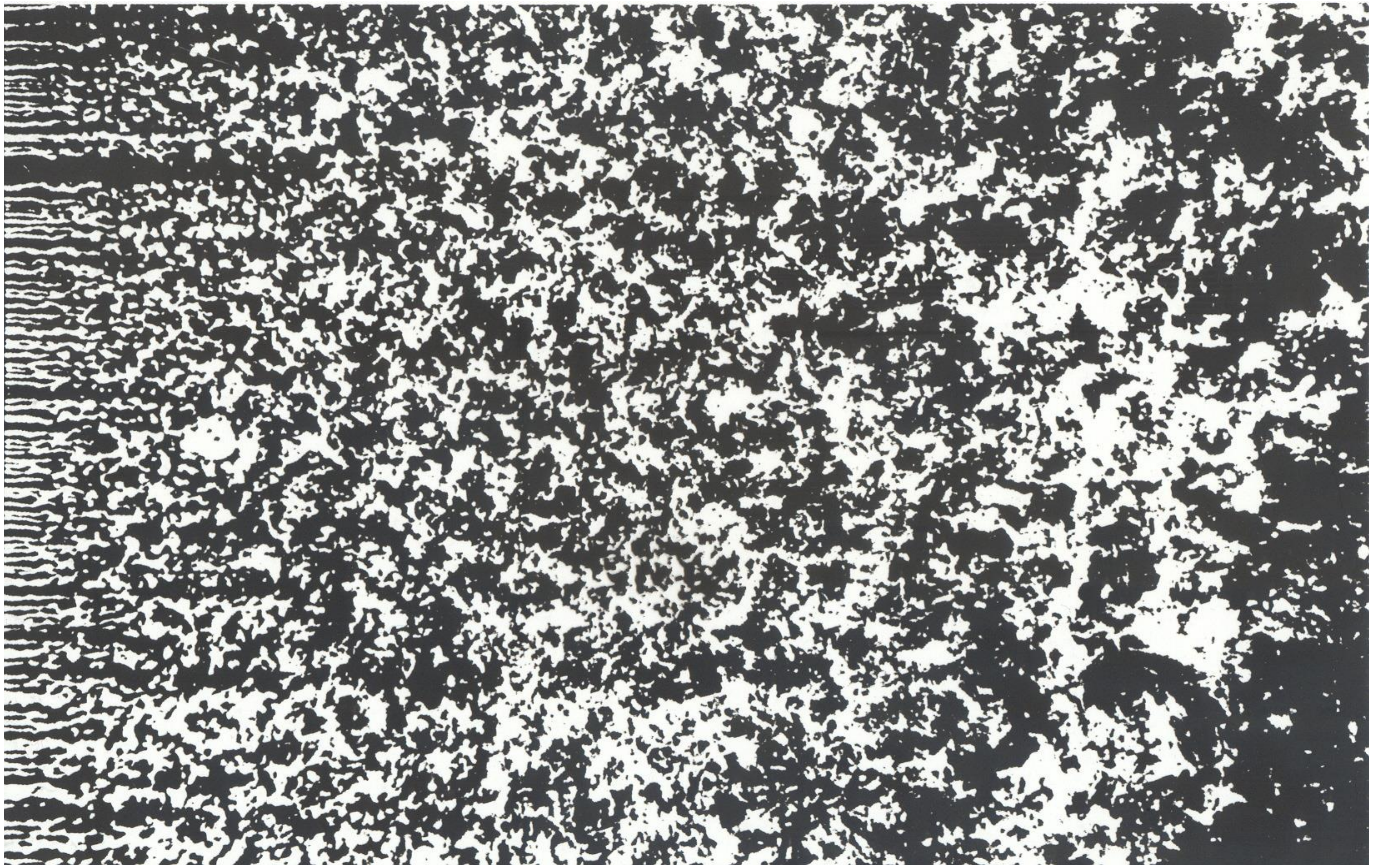

BOUNDARY LAYER ON A FLAT PLATE

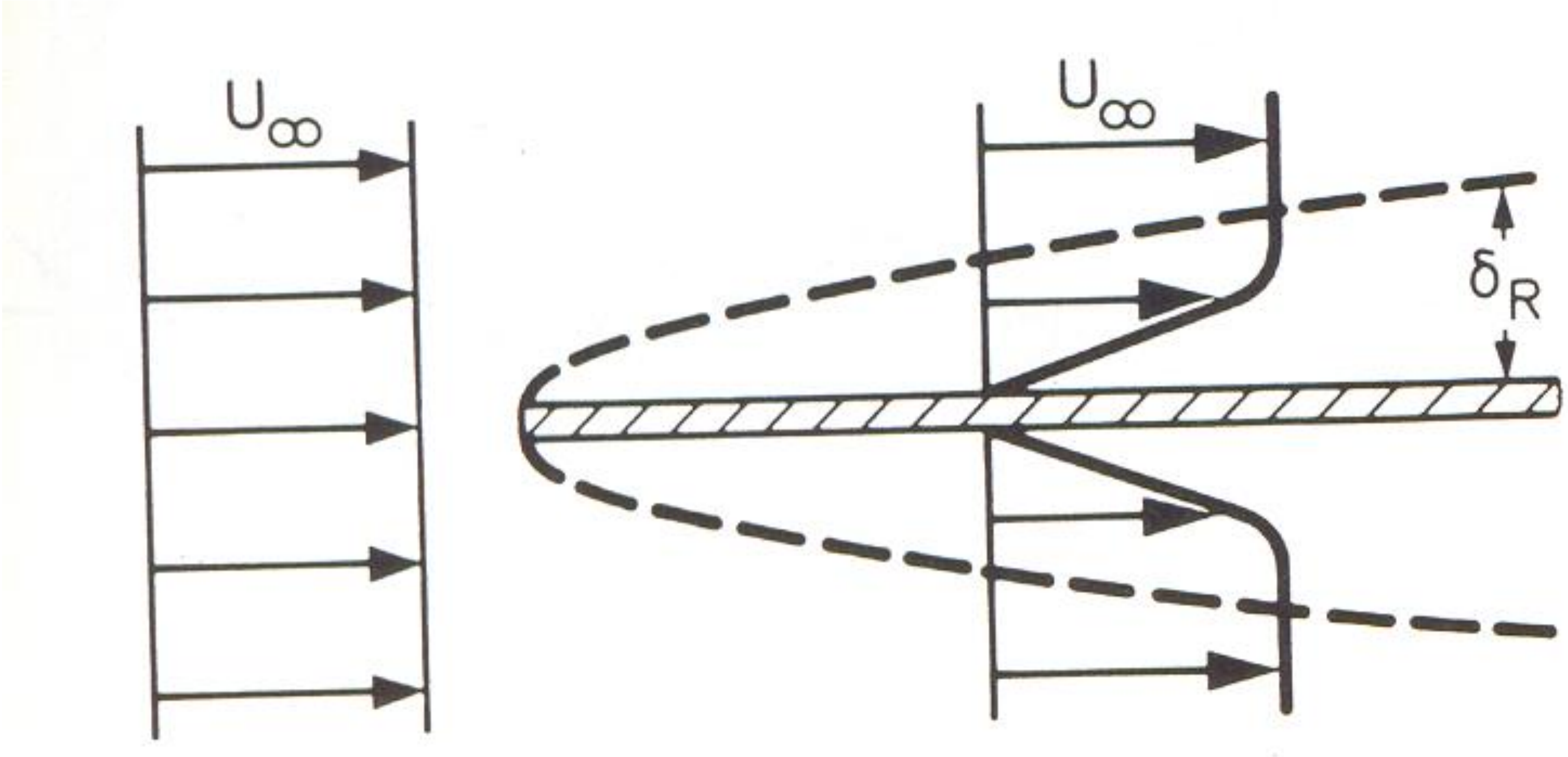

Plattengrenzschicht U_∞ = Anströmung,
δ_R = Reibungsgrenzschichtdicke

MODERN FLUID DYNAMICS WAS BORN HERE

Für das ebene Problem, das ich bisher allein behandelt habe, erhält man beim stationären Zustand (X-Richtung tangential, Y-Richtung normal, u und v die entsprechenden Geschwindigkeitskomponenten) die Differentialgleichung

$$\varrho\left(u\frac{\partial u}{\partial x}+v\frac{\partial u}{\partial y}\right)+\frac{dp}{dx}=k\frac{\partial^2 u}{\partial y^2};$$

dazu kommt noch

$$\frac{\partial u}{\partial x}+\frac{\partial v}{\partial y}=0.$$

Ist, wie gewöhnlich, $\frac{dp}{dx}$ durchaus gegeben, ferner für den Anfangsquerschnitt der Verlauf von u, so läßt sich jede derartige Aufgabe numerisch bewältigen, indem man durch Quadraturen aus jedem u das zugehörige $\frac{\partial u}{\partial x}$ gewinnen kann; damit kann man mit Hilfe eines der bekannten Näherungsverfahren*) immer wieder um einen Schritt in der X-Richtung weiterkommen. Eine Schwierigkeit besteht dabei allerdings in verschiedenen am festen Rande auftretenden Singularitäten. Der einfachste Fall der hier behandelten Bewegungszustände ist der, daß das Wasser an einer ebenen dünnen Platte entlang strömt. Hier ist eine Reduktion der Variablen möglich; man kann $u = f\left(\frac{y}{\sqrt{x}}\right)$ setzen. Durch numerische Auflösung der entstehenden Differentialgleichung kommt man auf eine Formel für den Widerstand

$$R = 1{,}1\cdots b\sqrt{k\,\varrho\,l\,u_0^3}$$

(b Breite, l Länge der Platte, u_0 Geschwindigkeit des ungestörten Wassers gegenüber der Platte). Den Verlauf von u gibt Fig. 1

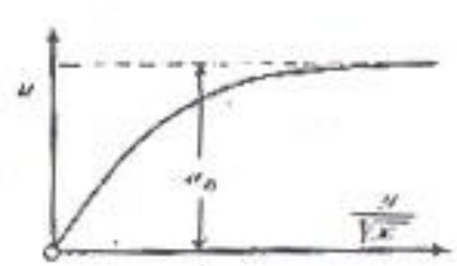

Fig. 1

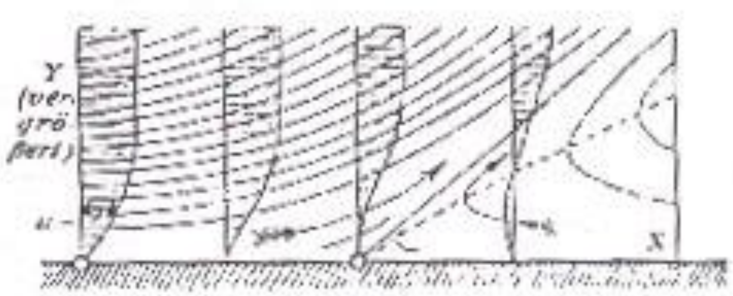

Fig. 2

The boundary layer idea made bridges between hydraulics and hydrodynamics

Prandtl 1904

Separating boundary layer

BOUNDARY LAYER SEPARATION : DYNAMIC STALL

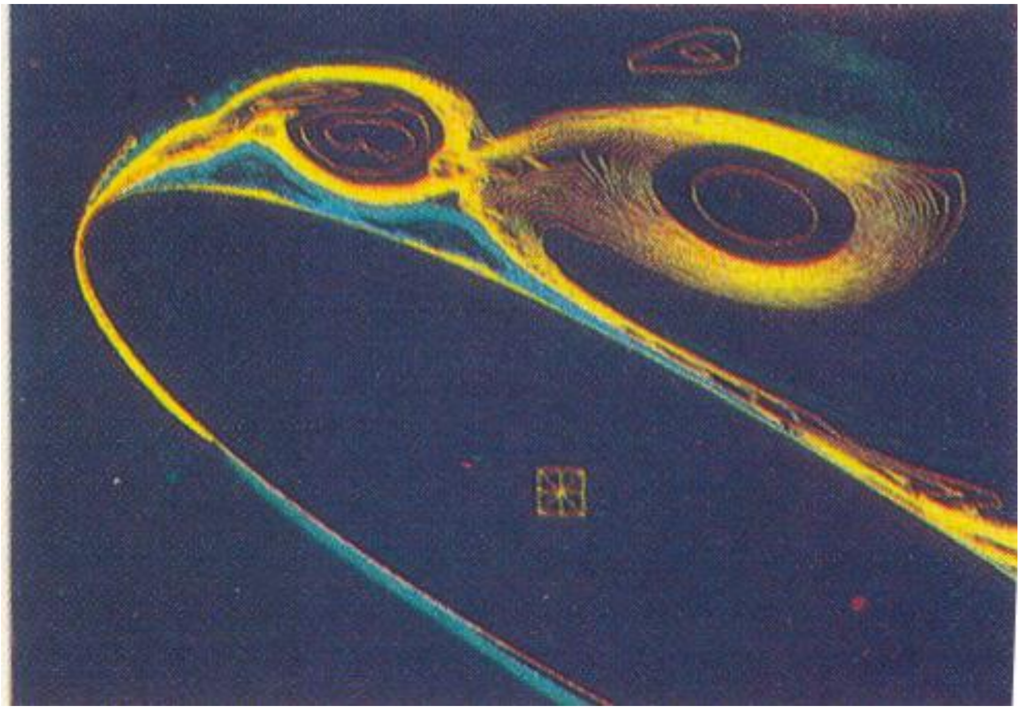

Computed instantaneous flow structure near the leading edge of a NACA 0015 airfoil as it is pitching up. Angle of attack = 28.56^0 (left), 29.71^0 (right), Re = 45 000.

Ghia + 1993

SEPARATION : FLOW PAST SPHERE

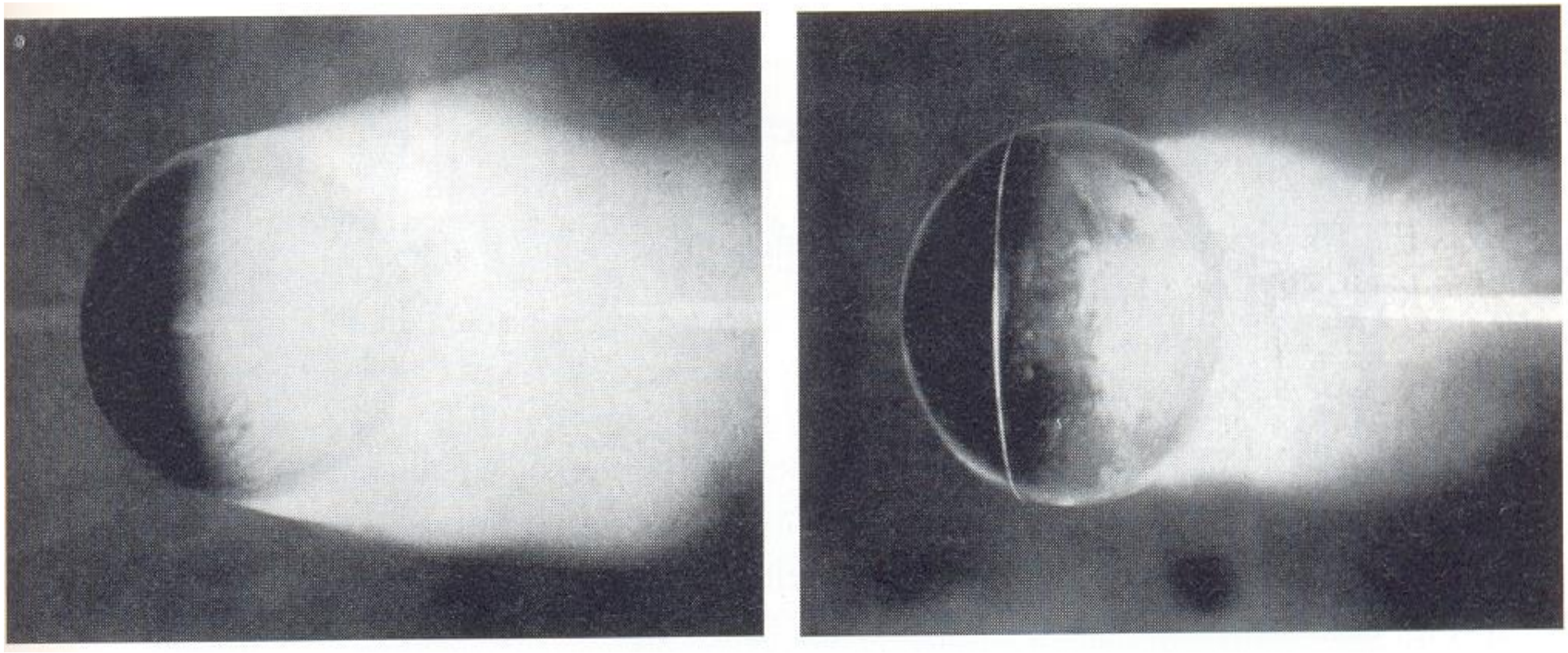

Prandtlscher Stolperdraht bei der Kugelumströmung
a) laminare Strömung, b) turbulente Strömung

BASE PRESSURE COEFFICIENT ON CYLINDER

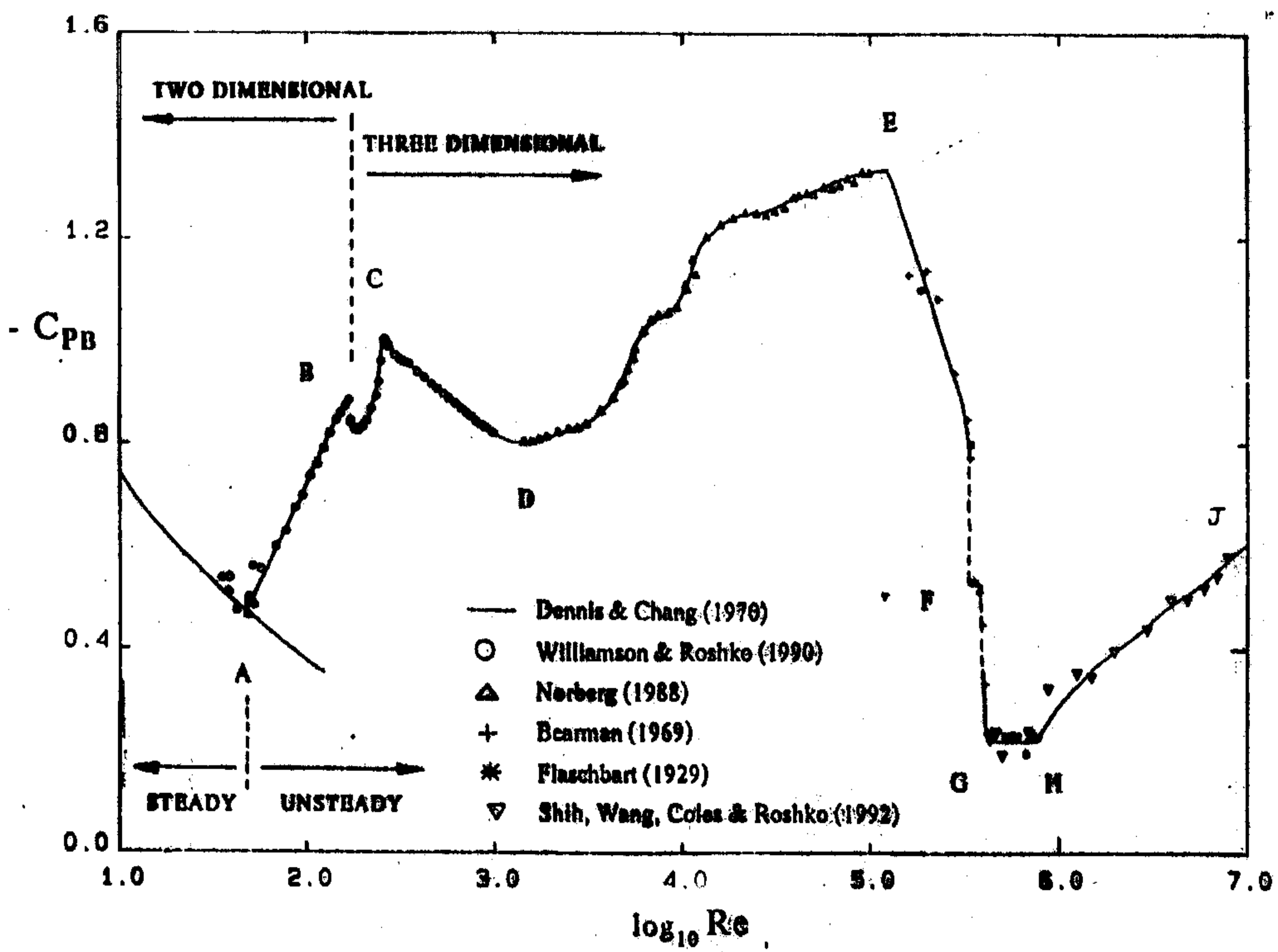

Variations of pressure coefficient at rear stagnation point on a circular cylinder with increasing Reynolds number

TRANSITION IN A PIPE : REYNOLDS' EXPERIMENT

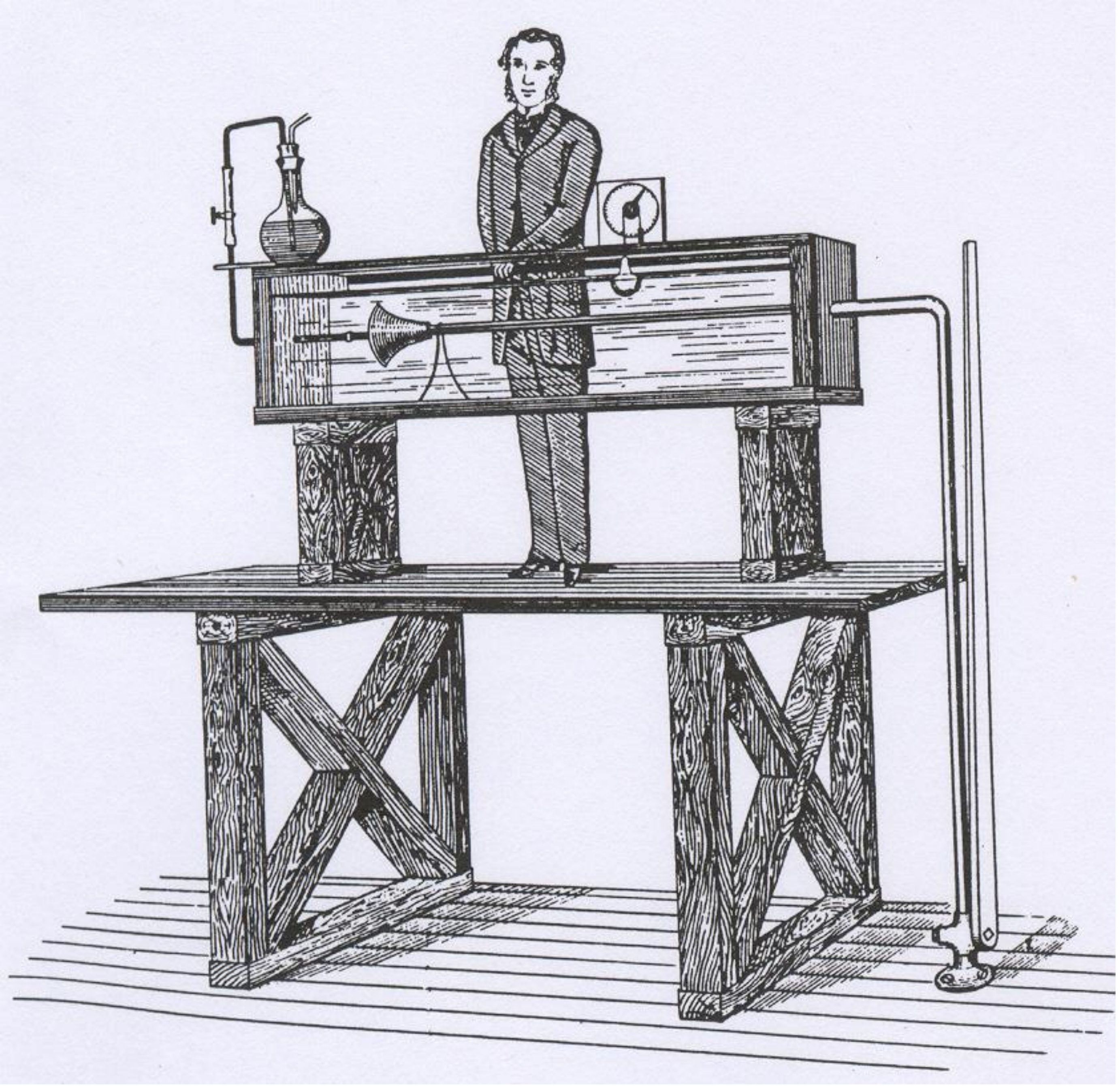

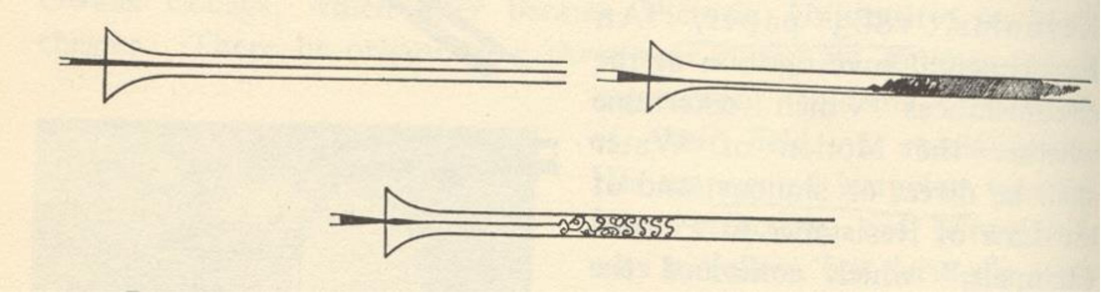

'Flashes' of turbulence

Rott N 1990*Annual Review Fl. Mech.* 22:1-11

TRANSITION IN PIPE / ON FLAT PLATE

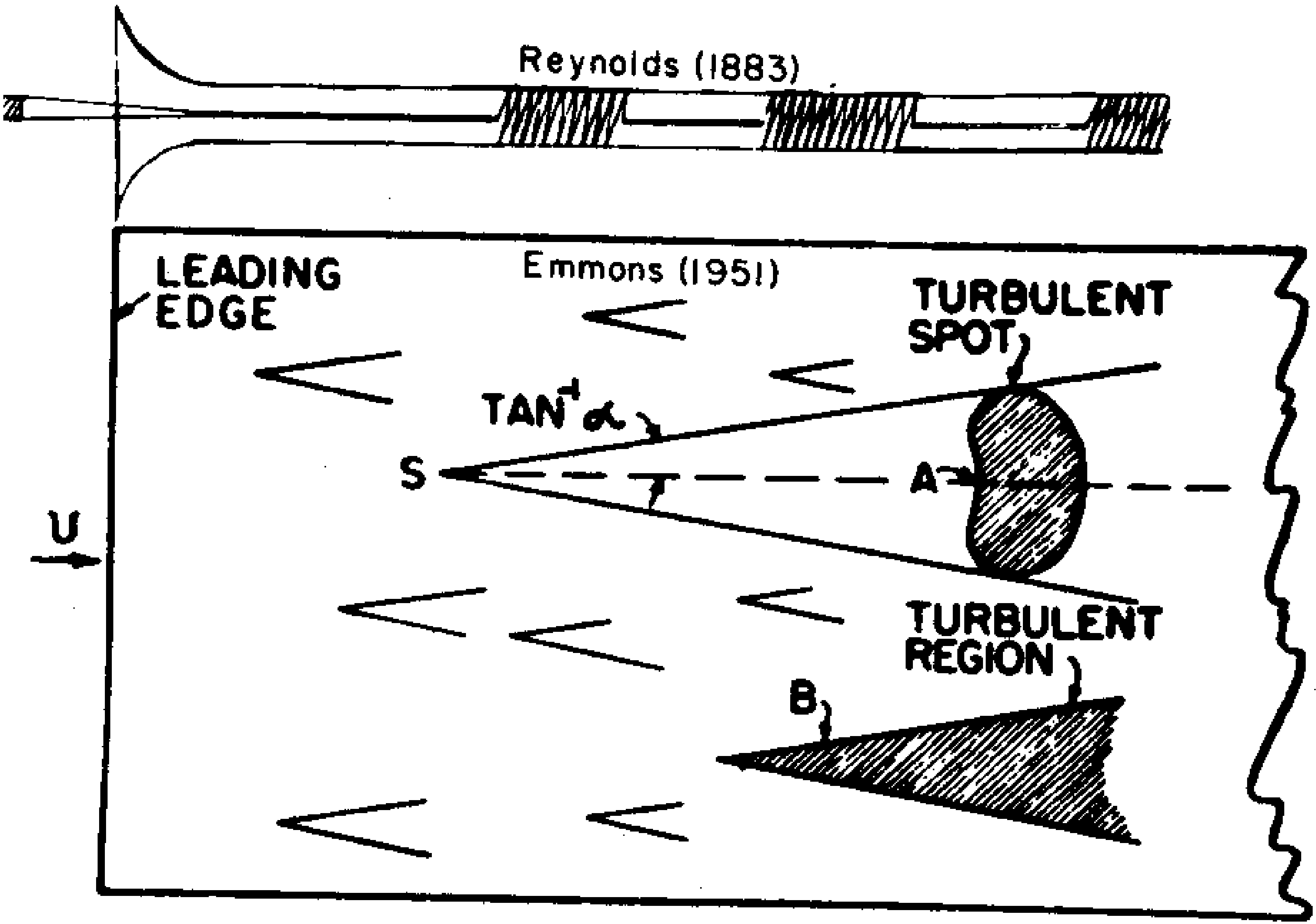

TRANSITION IN THE BOUNDARY LAYER ON A FLAT PLATE

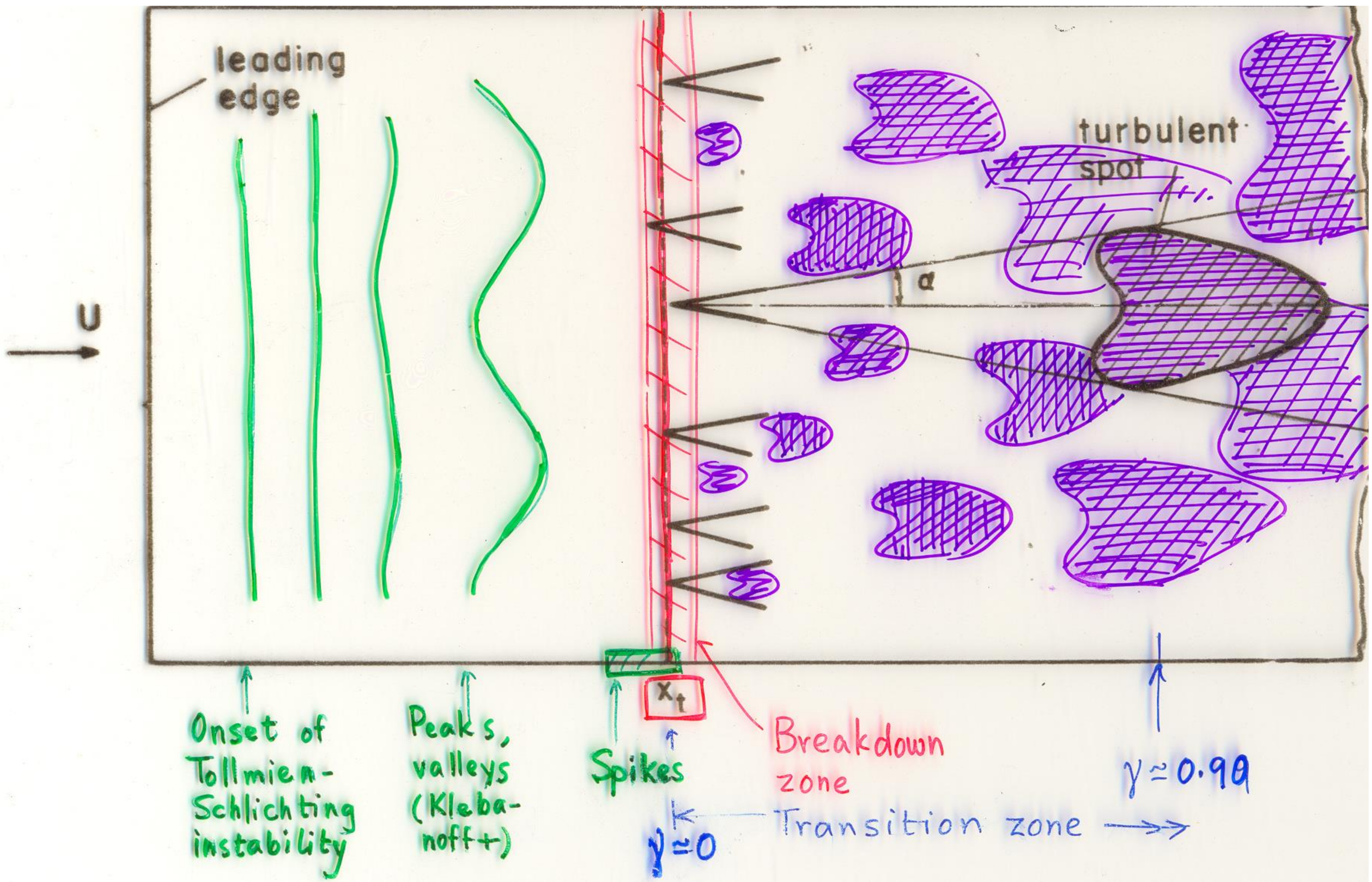

After RN 1957, Dhawan & RN 1958

TRANSITION ON A WING : SURFACE TEMPERATURE BY LIQUID CRYSTAL TECHNIQUE

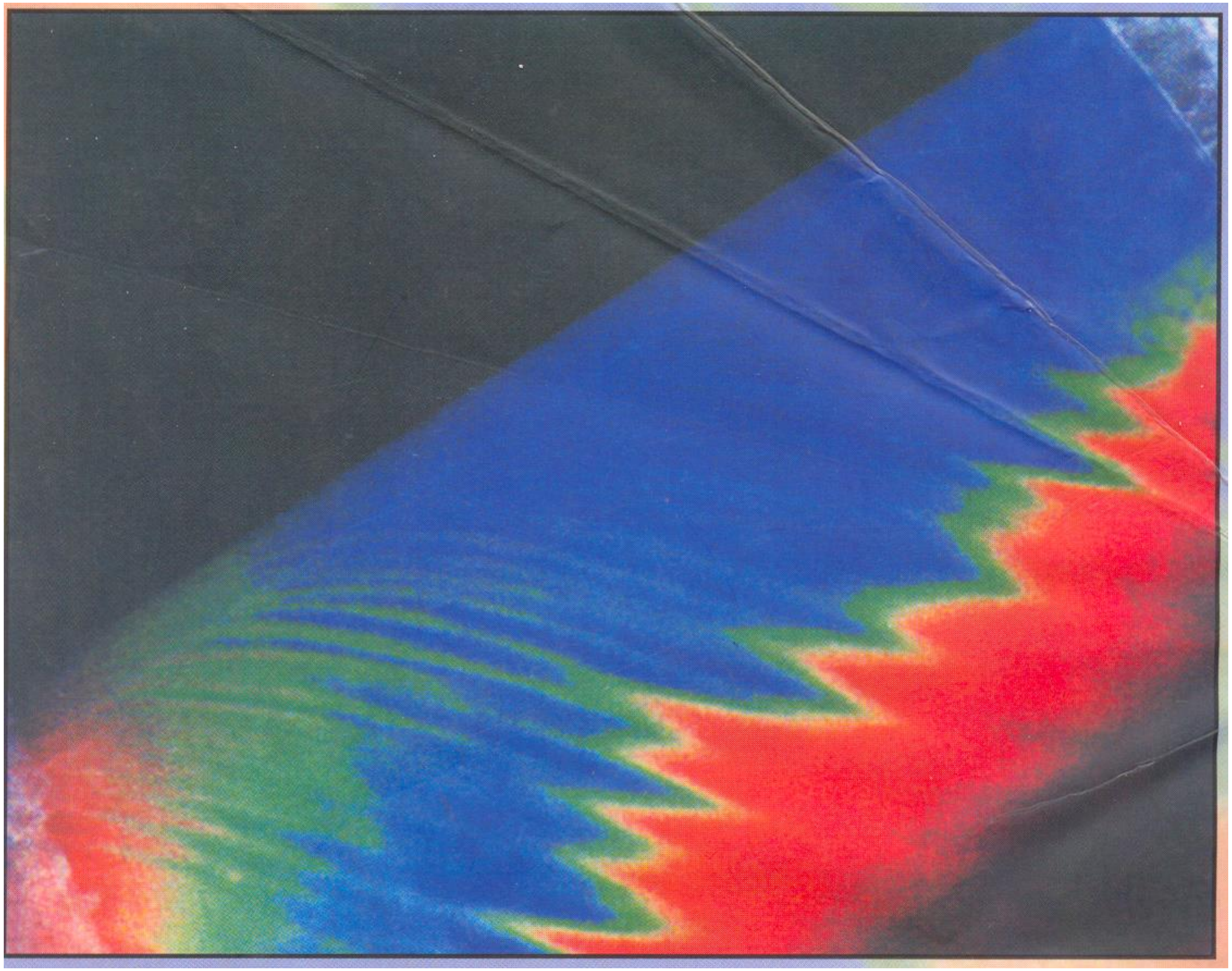

Sweep angle = 55°

Kohama 2000

TRANSITIONING CIGARETTE PLUME

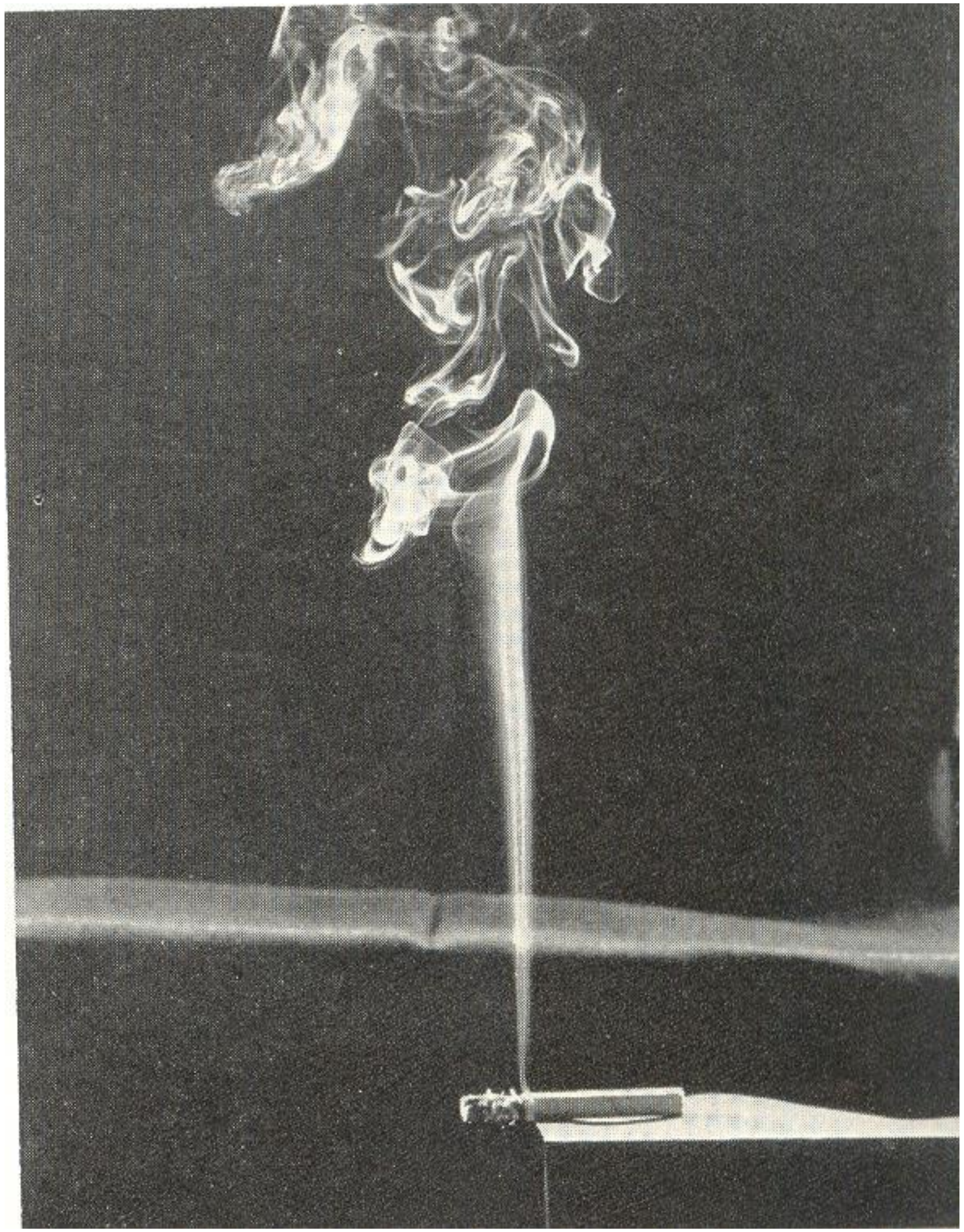

REVERSE TRANSITION

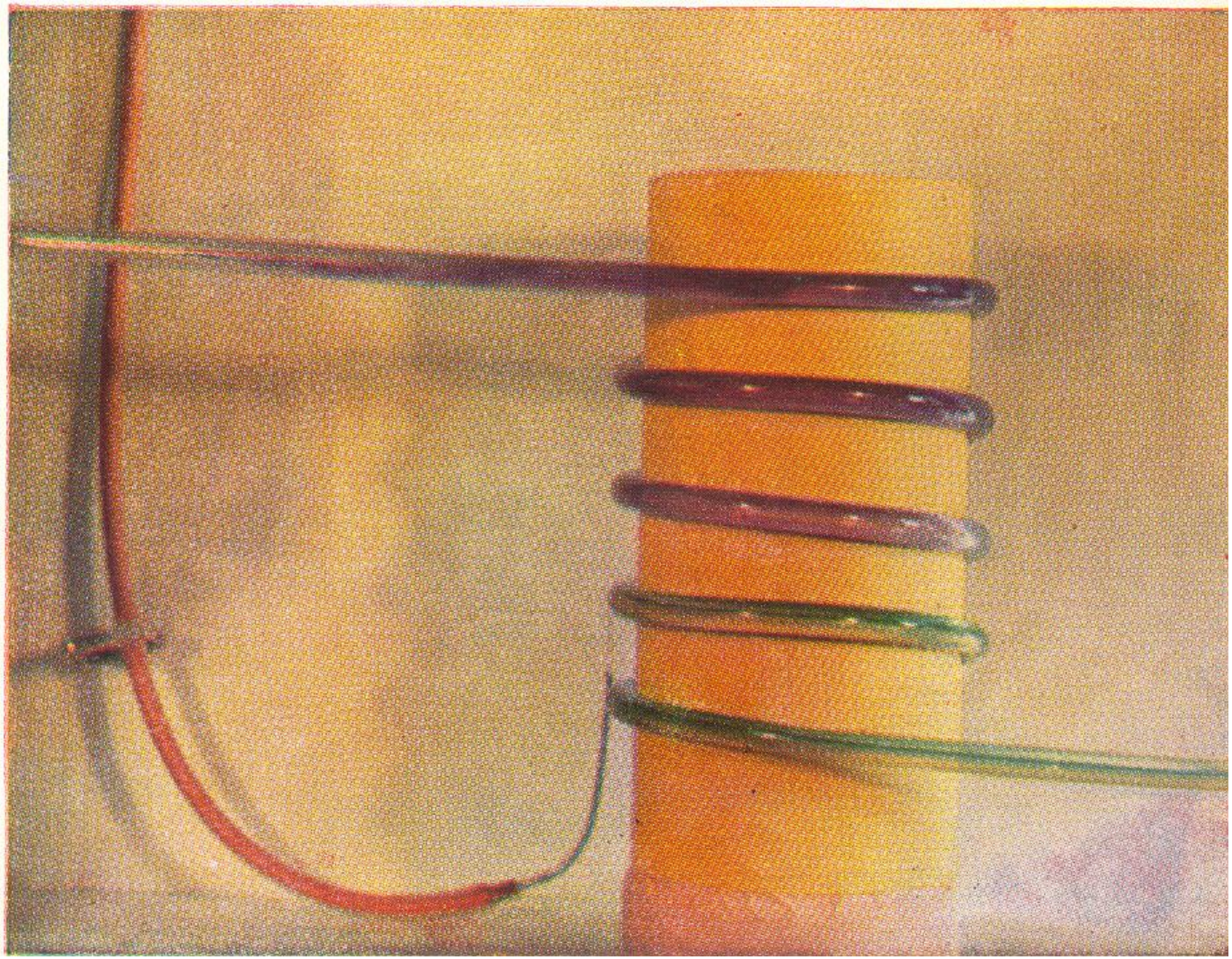

Reversion in a coiled tube

Viswanath P R et al.
1978 J. IISc 60:159-165

STABLE STRATIFICATION KILLS TURBULENCE

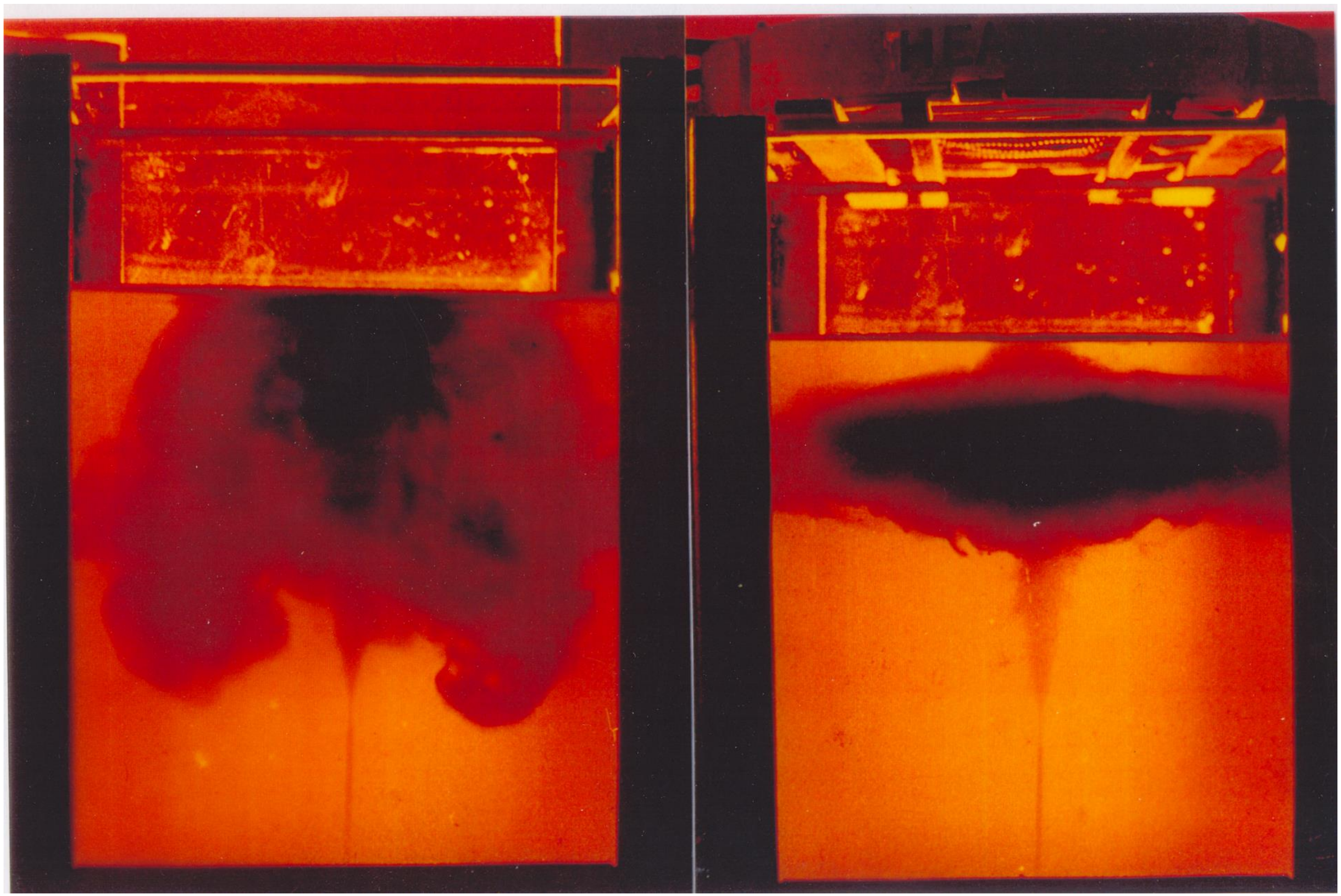

TRANSITION RELAMINARIZATION

P R Viswanath ++ 1978

RELAMINARIZATION IN SUPERSONIC EXPANSION

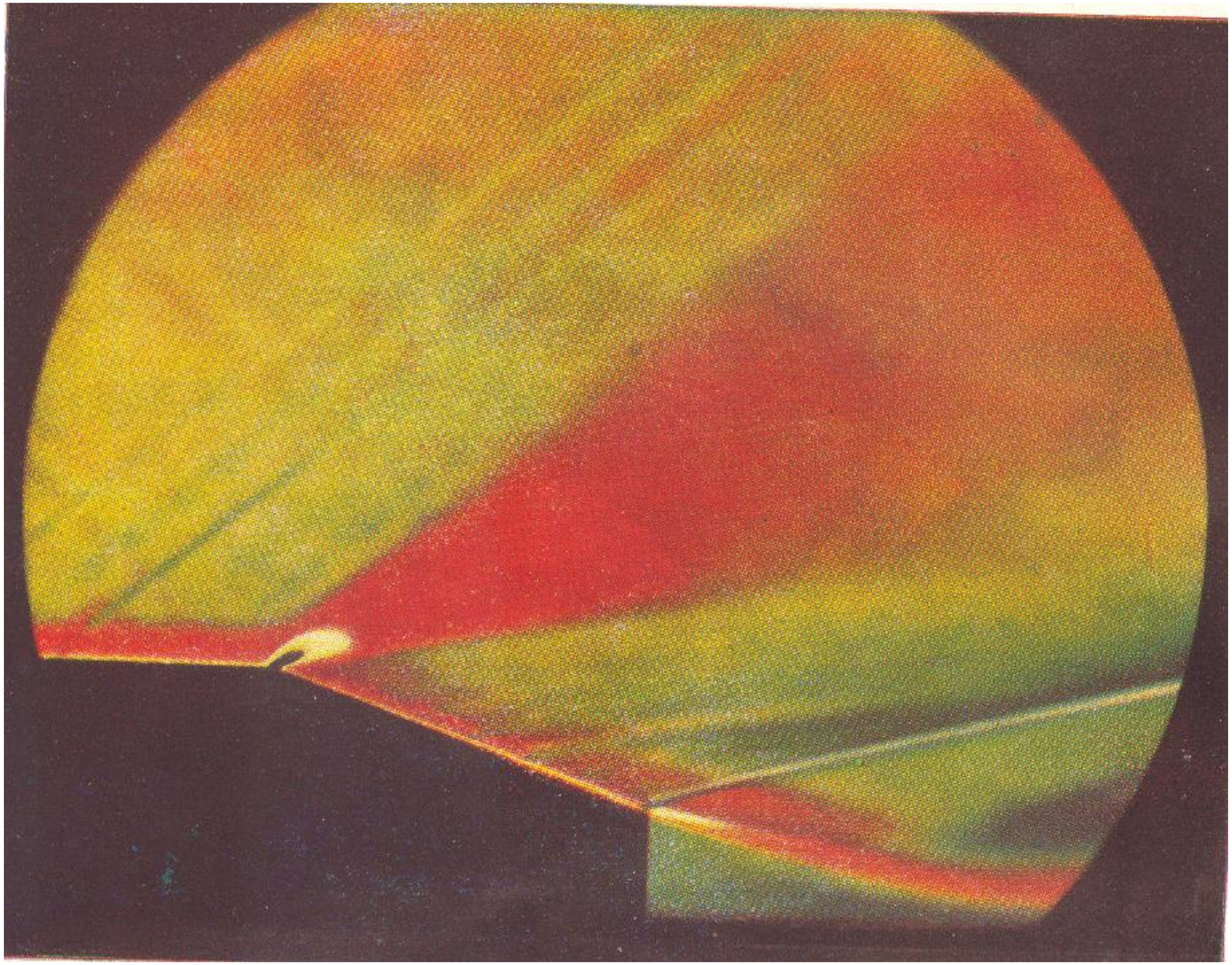

Relaminarization at an expansion corner in supersonic flow

Viswanath P R et al. 1978 J. IISc 60:159-165

RELAMINARIZATION IN A HIGHLY FAVOURABLE PRESSURE GRADIENT

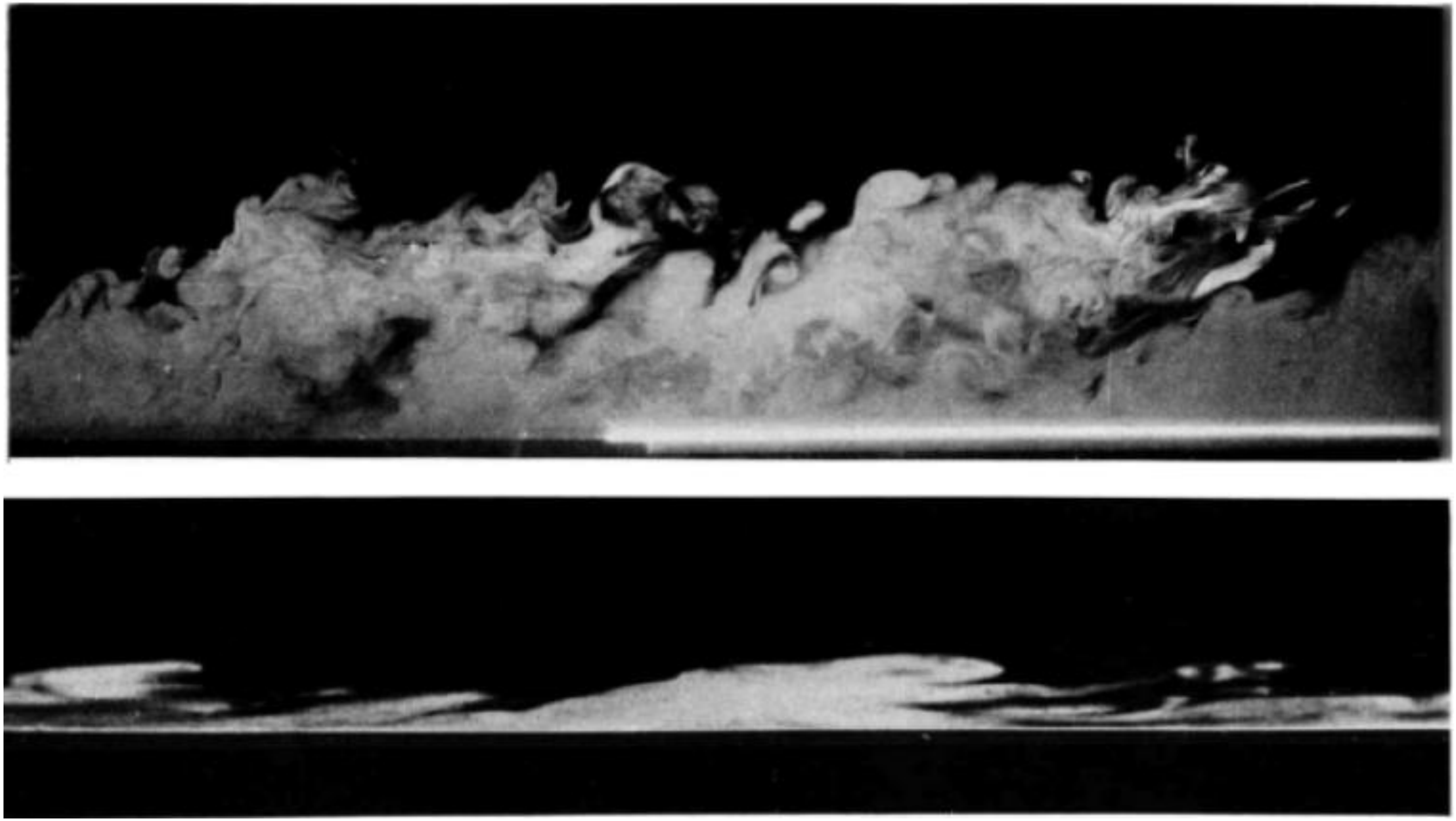

Upper: zero pressure gradient
Lower: highly favourable pressure gradient
Falco 1977, 1982 from Van Dyke 1982

FLOW REGIMES IN REVERTING BOUNDARY LAYER SUBJECTED TO ACCELERATION

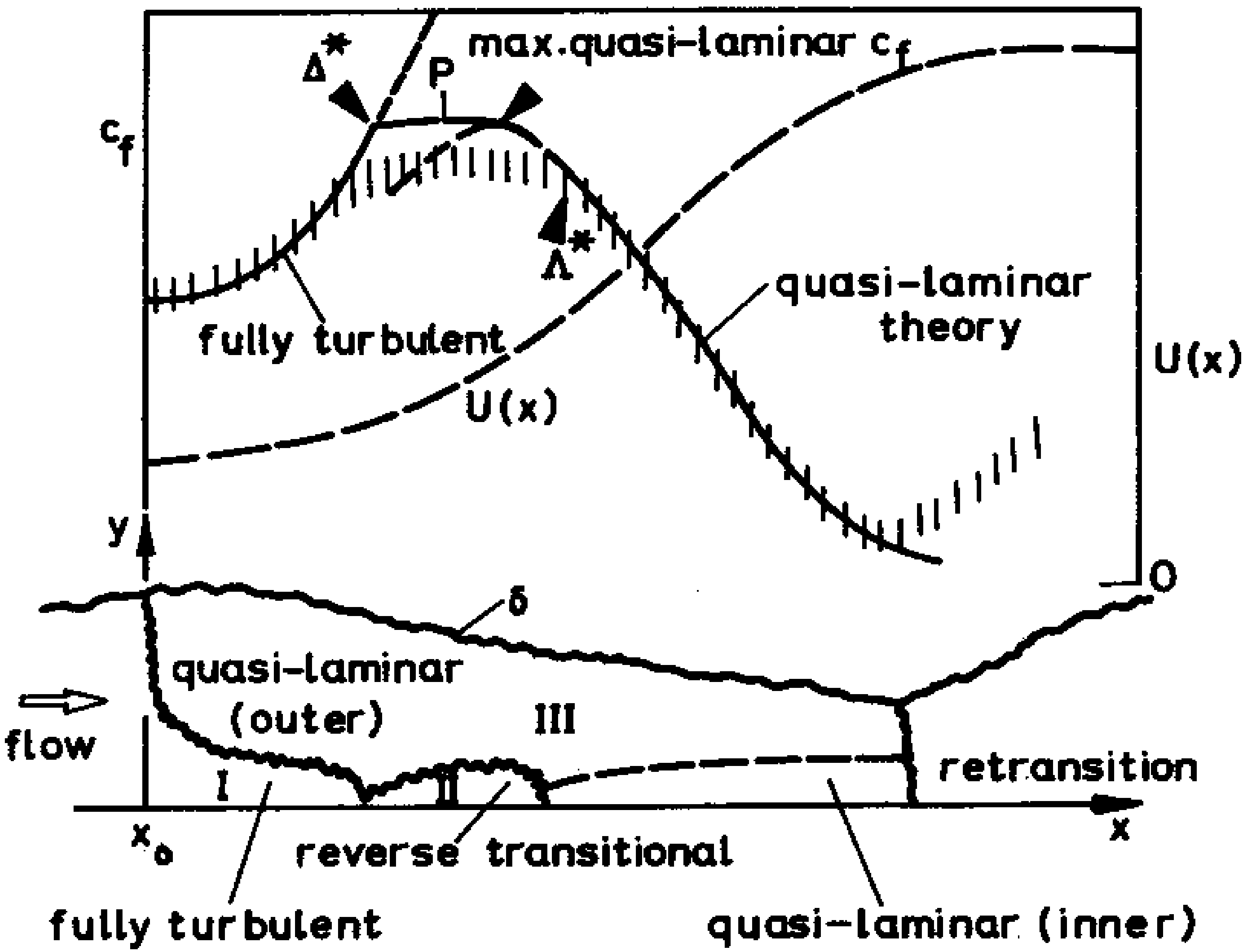

R Narasimha, K R Sreenivasan 1973 JFM

ORDER IN TURBULENT MIXING LAYER

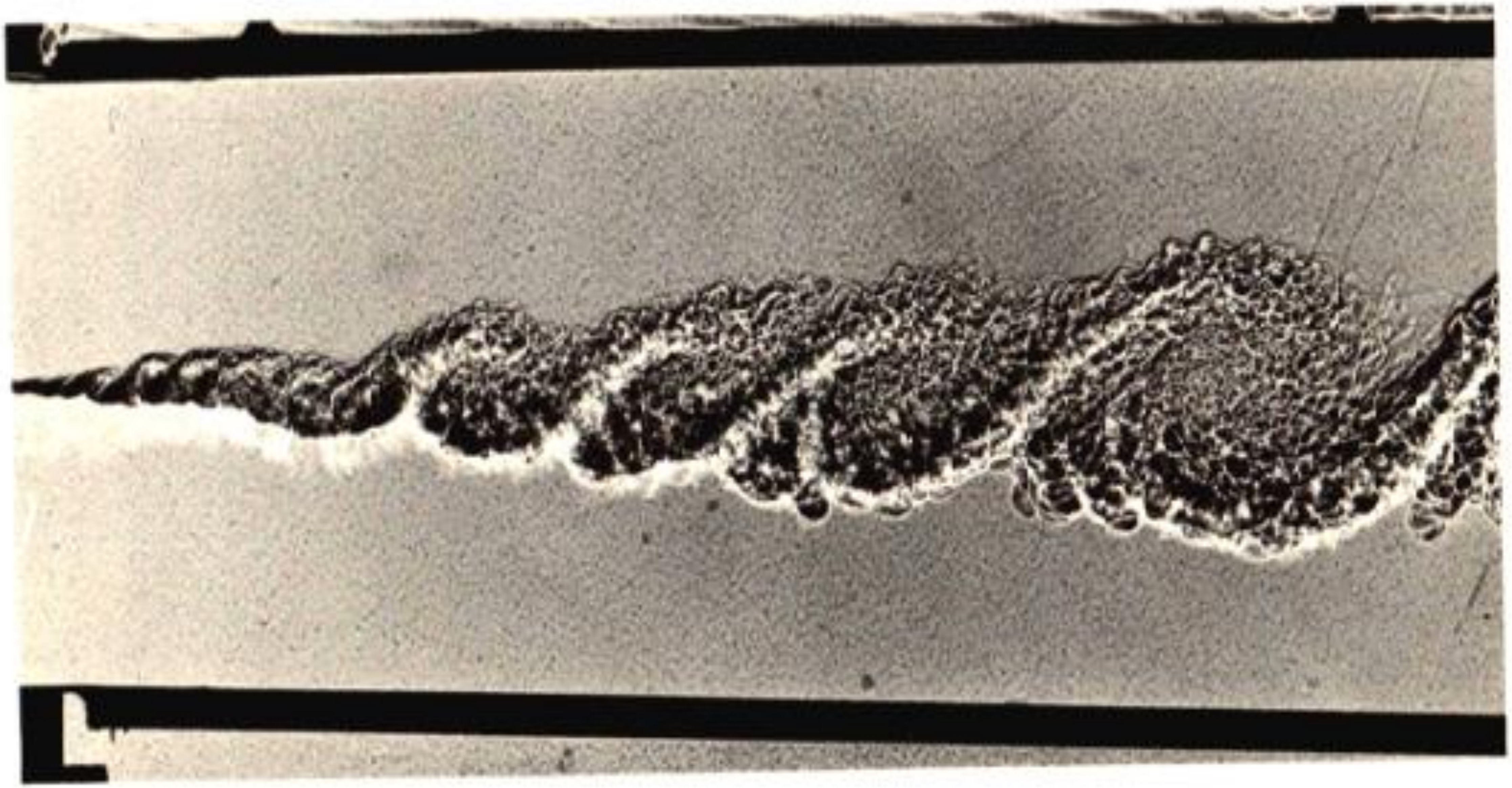

Figure 1. Spark shadowgraph of mixing layer between helium (upper) with U_1 = 1010 cm/sec and nitrogen (lower) with U_2 = 380 cm/sec. Pressure = 8 atm.

Spark shadowgraph of mixing layer between helium (upper) with U_1 = 1010 cm/sec and nitrogen (lower) with U_2 = 380 cm/sec. Pressure 8 atm. Brown & Roshko 1971

ORDER IN PLUME FLOW BY WAVELET TRANSFORM

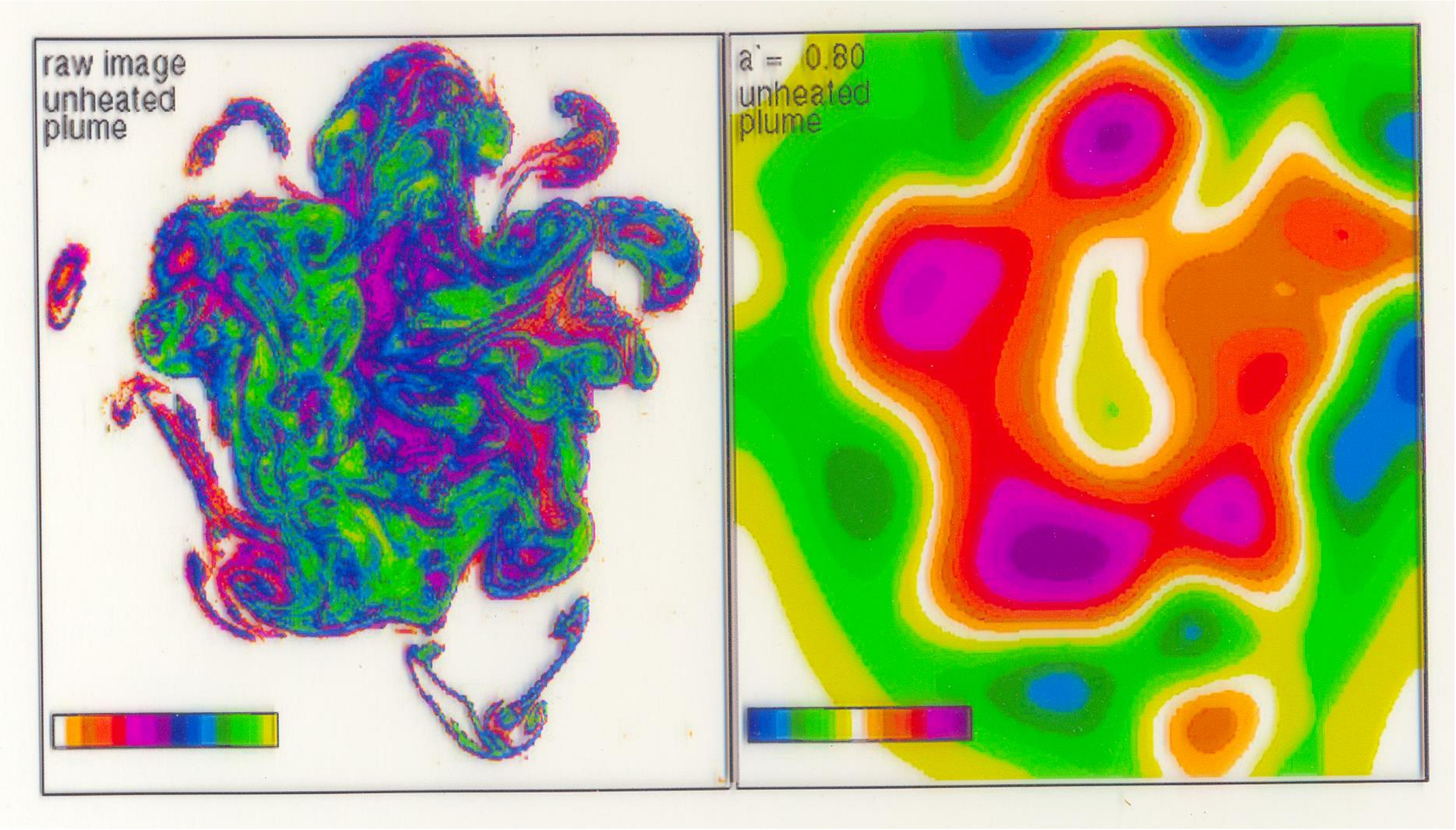

RN et al. 2002

ISLAND SHEDS KARMAN VORTICES?

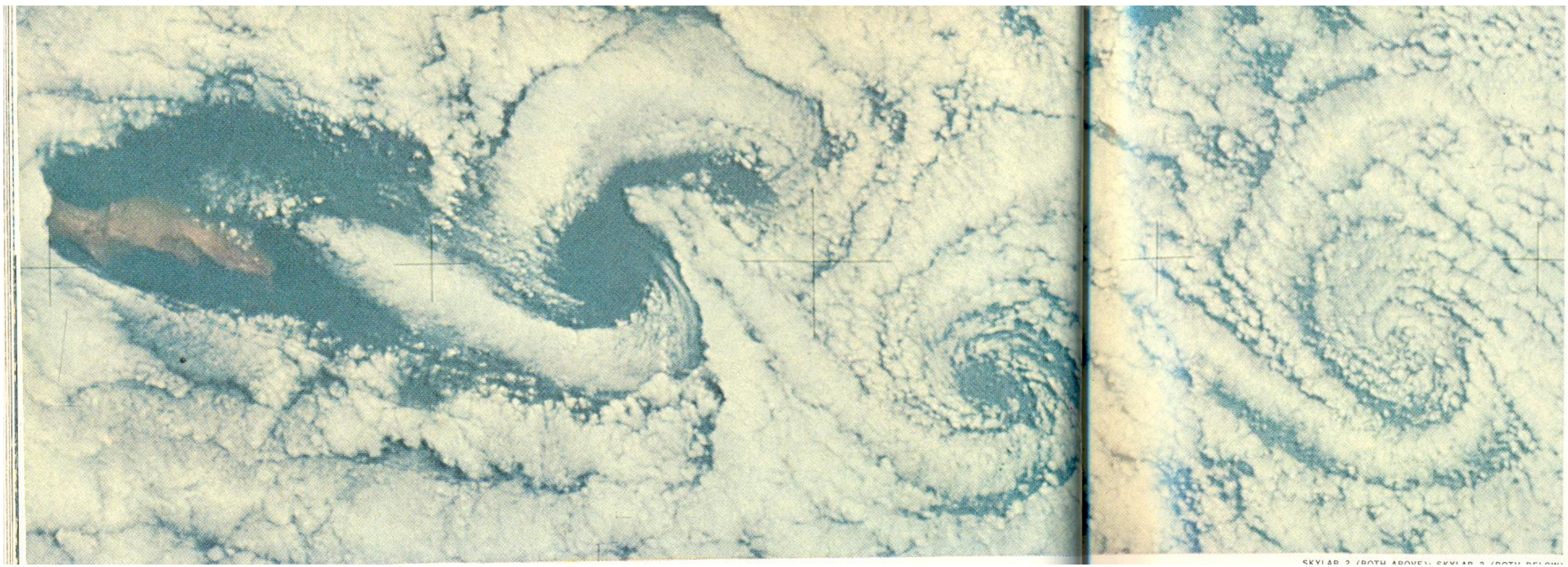

THE BLIND MEN AND THE TURBULENT ELEPHANT

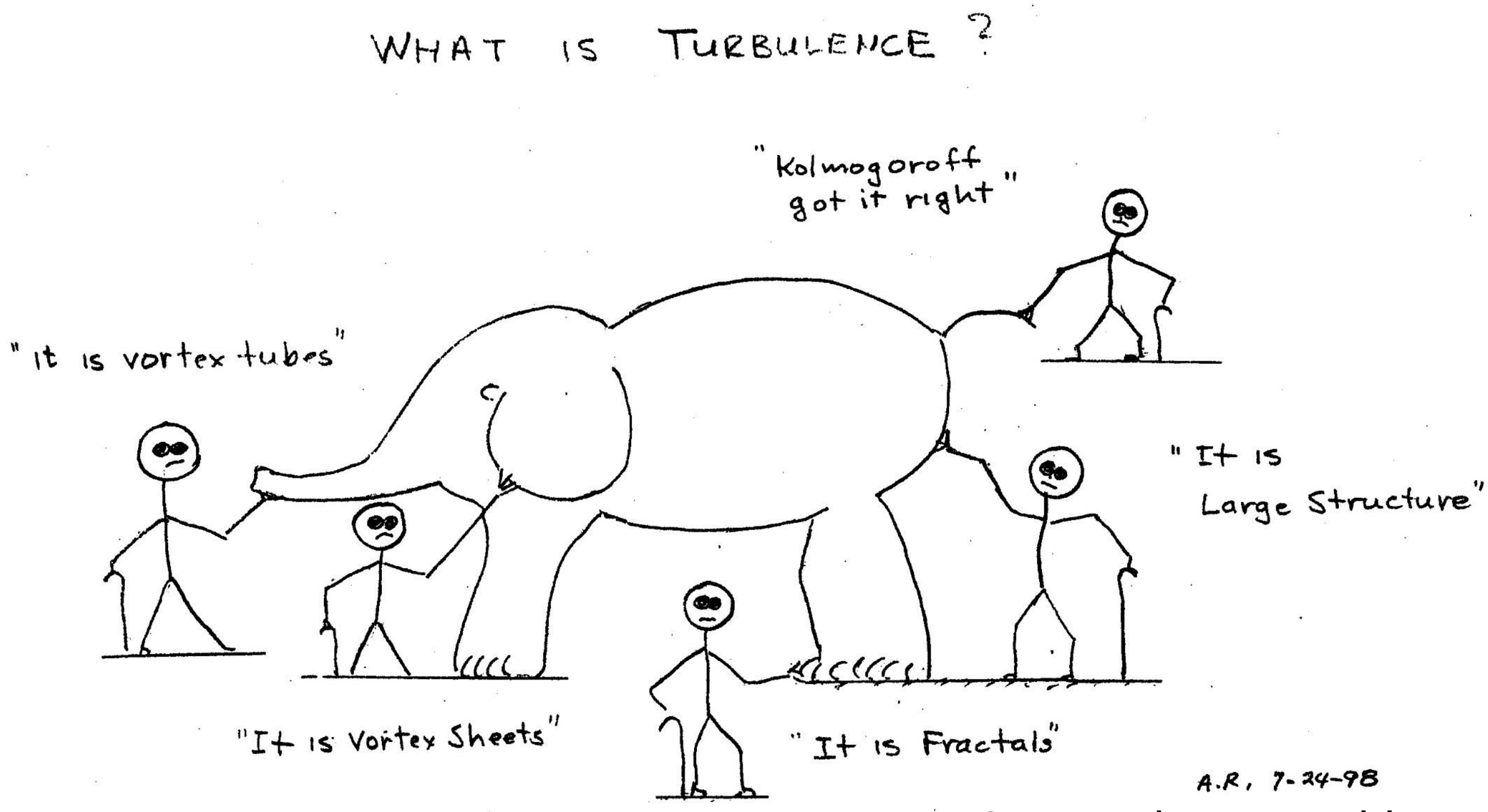

Cartoon by A. Roshko

Wild Life in the Flow Zoo on a Gas Turbine Blade

A Gas Turbine Engine

The most complex product in mechanical engineering

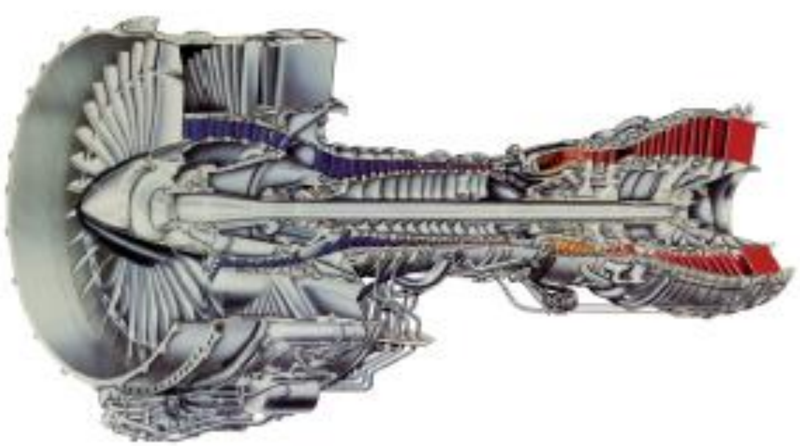

PW2000 engine (wiki)

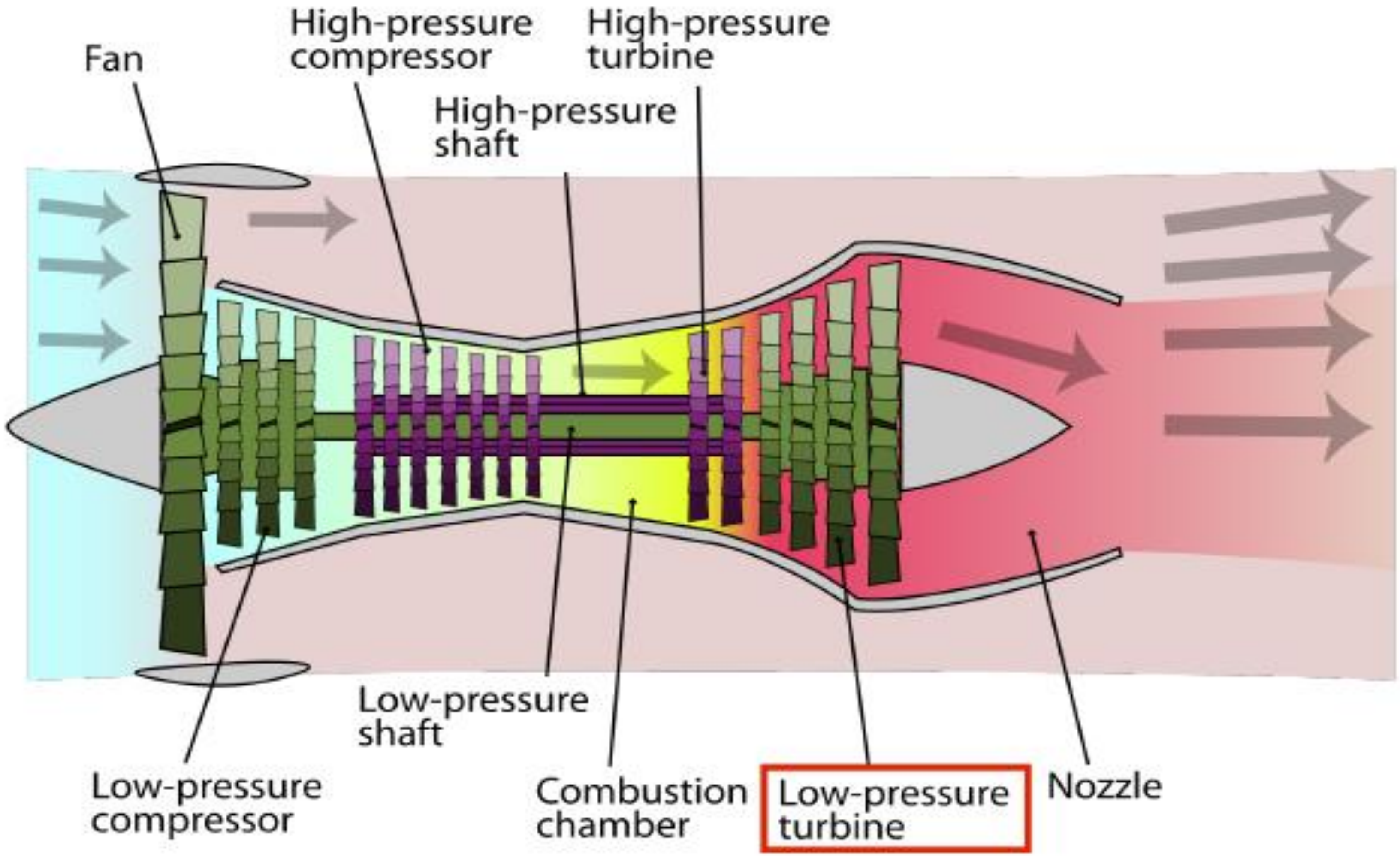

Schematic cross-section of high-bypass turbofan engine (wiki)

On Boeing 757, dual spool, bypass ratio 5.9:1
Thrust = 165-190KN   Dry weight = 3.22T
Blade temperatures of order 1500 C

The Wild Animals

Transition, relaminarization, separation, high curvature, highly-disturbed environment, rotation, hot blade surfaces . . .

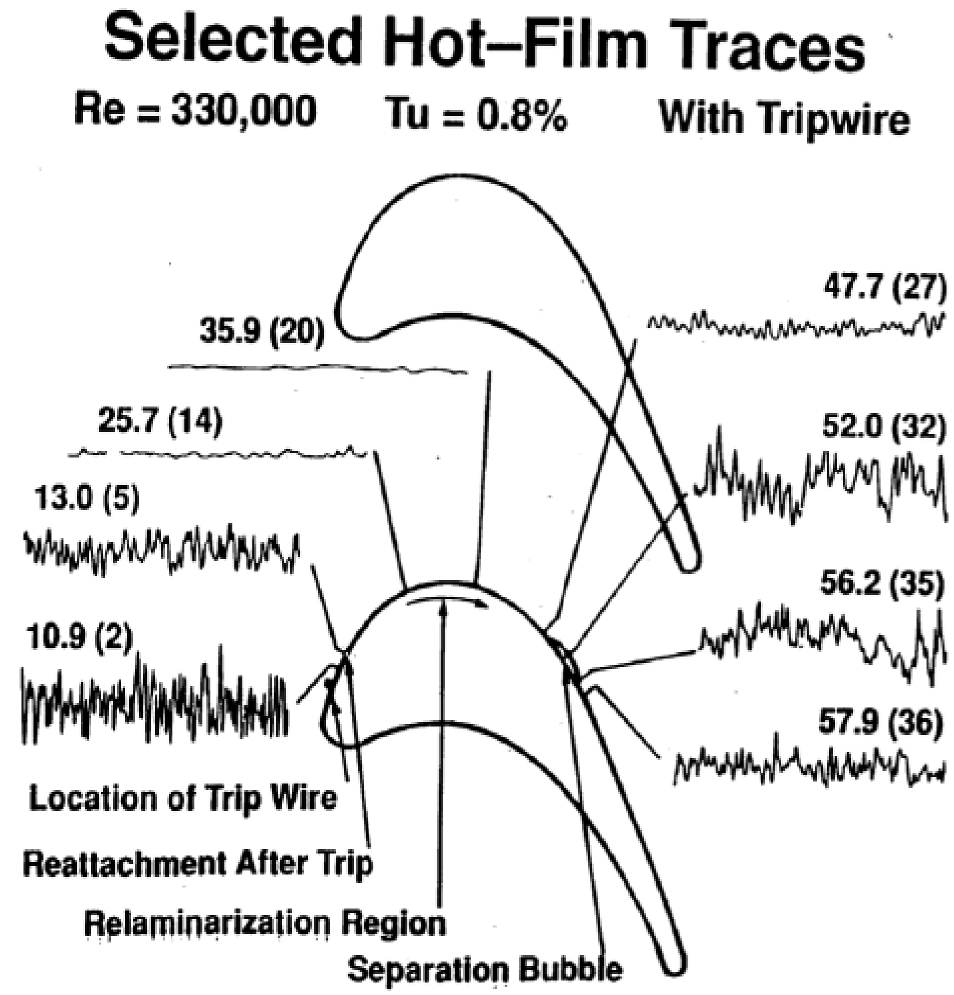

Wisler (1993)

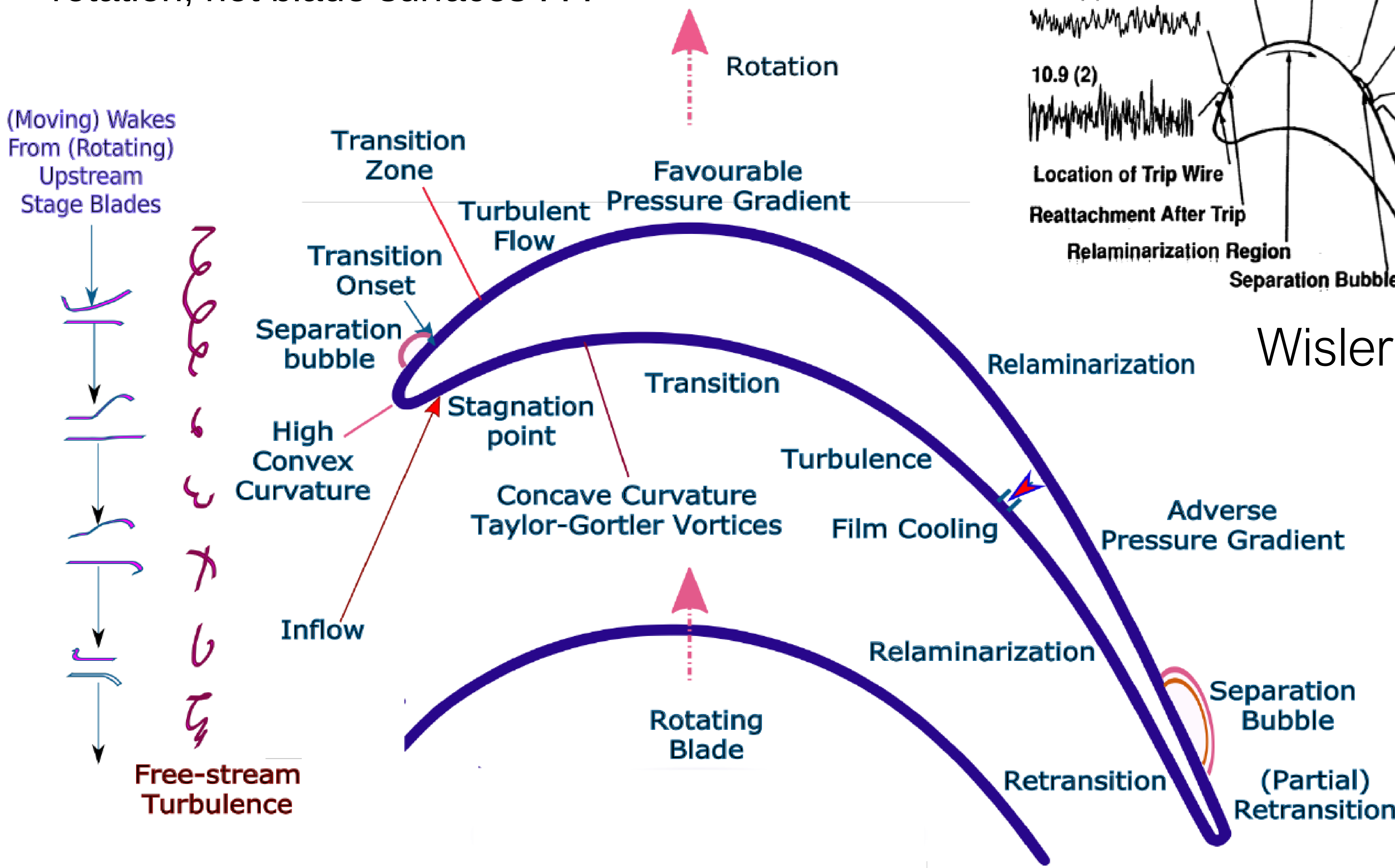

THE PROBLEM

- Blades operate in highly turbulent environment, often with a strong periodic component due to wakes from upstream rotor blades
- Strong pressure gradients and high surface curvature
- Blade Re ~20×10^3 to 1×10^6 : a modest but awkward range
- Blade boundary layer may experience transition, relaminarization and separation - all still beyond current RANS models
- Spatial and temporal variation of surface heat transfer rates by factor ~10
- A 25% difference in heat transfer rates on a turbine blade can mean an order of magnitude difference to its life.
- " 1% improvement in the efficiency of a low pressure turbine would result in a saving of $52,000 per year on a typical airliner." - Jahanmiri (2011)

- DNS possible at lower end of Re range (as of now)

Experimental studies in open literature

Ref	Blade	Re	Remarks
Stadtmuller (2002a,b)	T106A & T106D	60,000 & 500,000	Experimental data at low Re for wake-induced transition. Separation at TE
Stieger et al. (2003); Stieger & Hodson (2004, 2005)	T106A	160, 000	At low Re and low FSTI, wake triggers K-H instability that breaks into turbulent flow, gets convected
Liu & Rodi (1994b,a)	MTU	72,000	BL on suction side goes transitional under sweeping wakes. Higher wake-passing freq. raises heat transfer
Volino (2002a,b, 2003)	Pak-B	25,000-300,000	Increasing Re, FSTI move transition upstream. No reattachment and no transition at low Re
Choi et al. (2004)	-	15,700-105,000	Flow-separation at LE enhanced as Re decreases, suppressed by increasing FSTI
Kumaran et al. (2014), NAL	Typical Small Turbo Fan Engine (STFE)	152,000-1,000,000	Transition and relaminarisation cycles

Direct Numerical Simulation (DNS) Studies in Literature

Authors	Blade	Re	N=Nx×Ny×Nz	N×10^6
Wu & Durbin (2001)	T106A	148,000	1,152×384×128	56
Michelassi et al. (2002)	T106A	51,800	1,014×266×64	17
Kalitzin et al. (2003)	T106A	148,000	1,152×576×128	85
Wissink (2003)	T106A	51,831	1, 014×260×64	17
Wissink et al. (2006)	T106A	51,800	1,014×260×64	17
Wissink & Rodi (2006)	MTU	72,000	1,254×582×128	93
Ranjan et al. (2013, 2016)[1]	T106A	51,831	1,257,162×128	160
Michelassi et al. (2015)	T106A	59,634	274,176×66	18
Garai et al. (2015)	T106A	60,000	-	30.72
Maruthi et al. (2017)	STFE	152,000	733,841×128	93

[1]First compressible solution

DNS on T106A blade

Computational domain and simulation parameters for T106A[1]

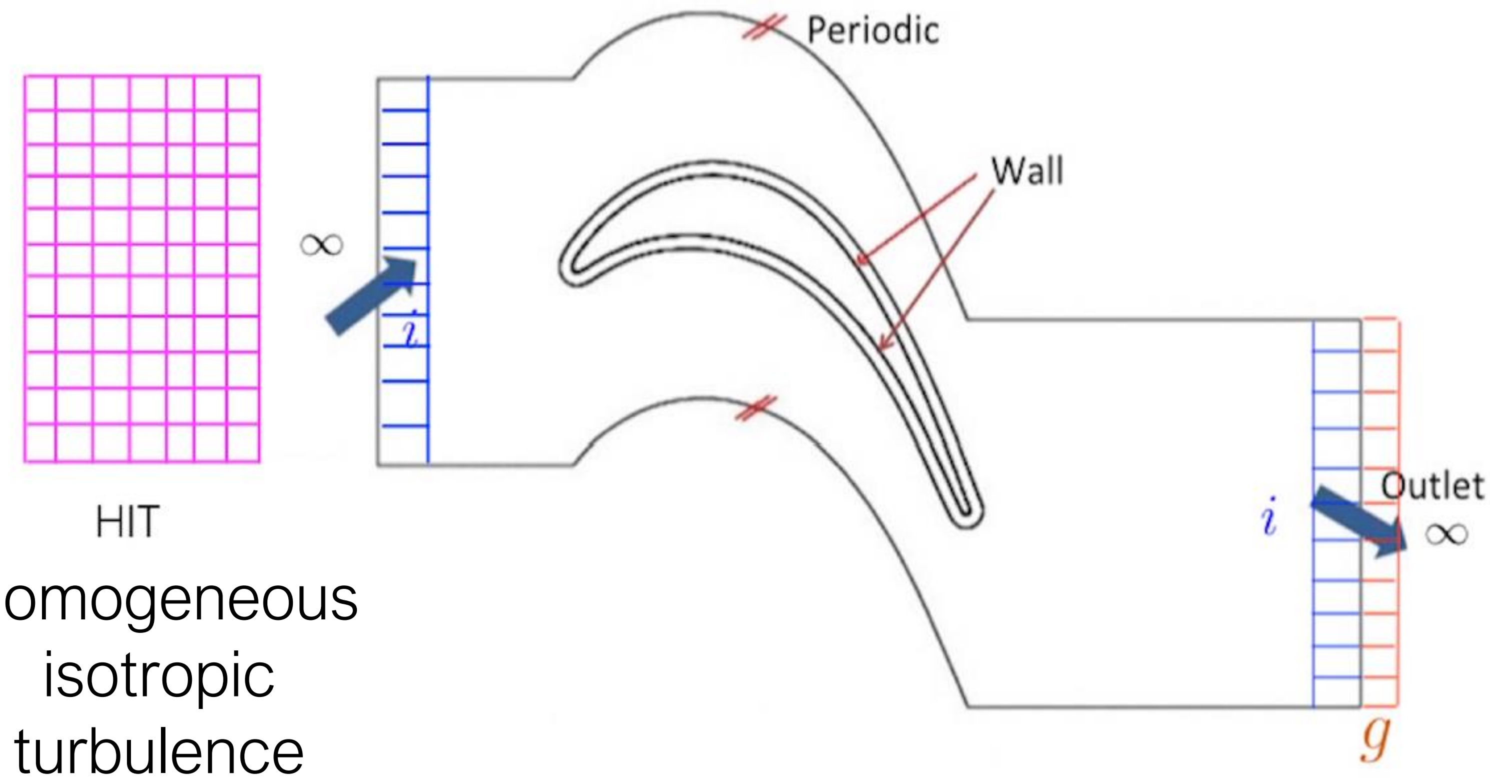

Homogeneous isotropic turbulence

Flow parameters

- $Re = 51831$
- $M = 0.1$ (inlet)
- $Pr = 0.71$
- $\beta_1 = 45.50^0$ (inlet AoA)

Simulation parameters

- CFL ≈ 1
- FSTI ≈ 0 – 10%
- Solution of previously simulated HIT (data due to Wu & Moin, JFM2009)
- Viscous padding near outflow
- 7-10 flow units

Sim	N_f	N_z	Grid Size
A	384,164	64	25×10^6
B	740,088	64	47×10^6
B1	740,088	128	95×10^6
C	1,257,162	128	161×10^6

Overview of simulations

[1]Ranjan++ 2017 Comp. Fluids

High-resolution compressible DNS on T106A

Leading edge

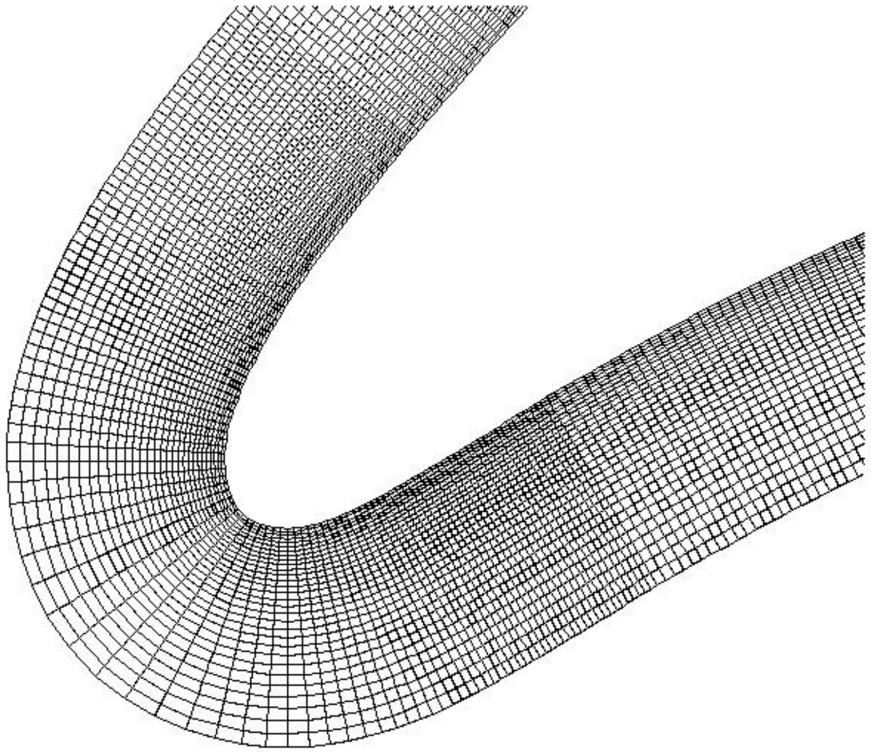

Trailing edge

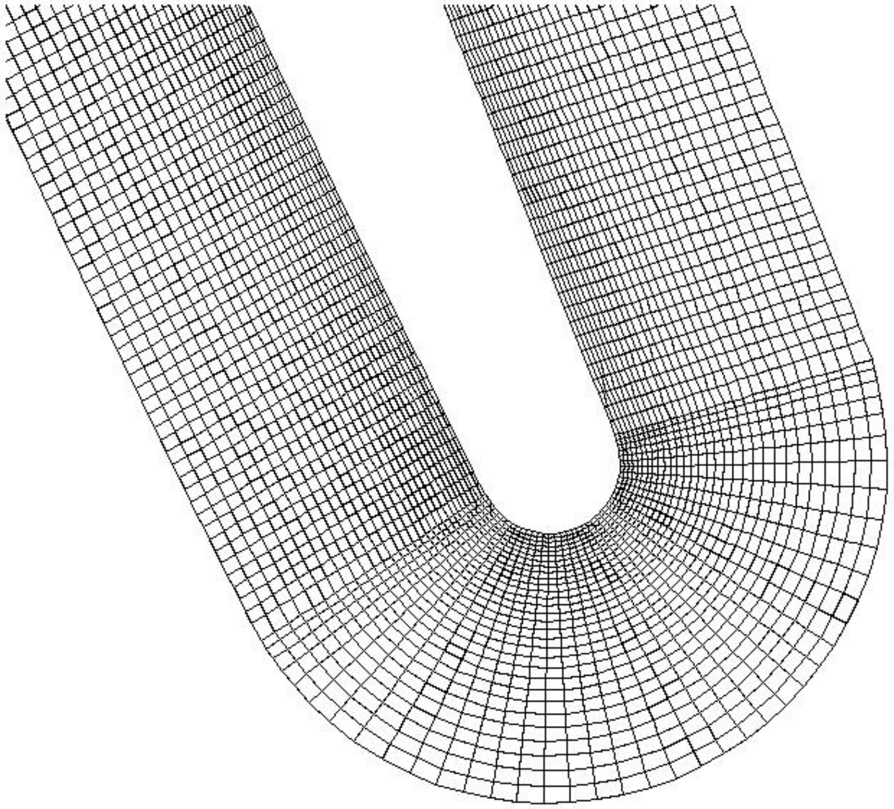

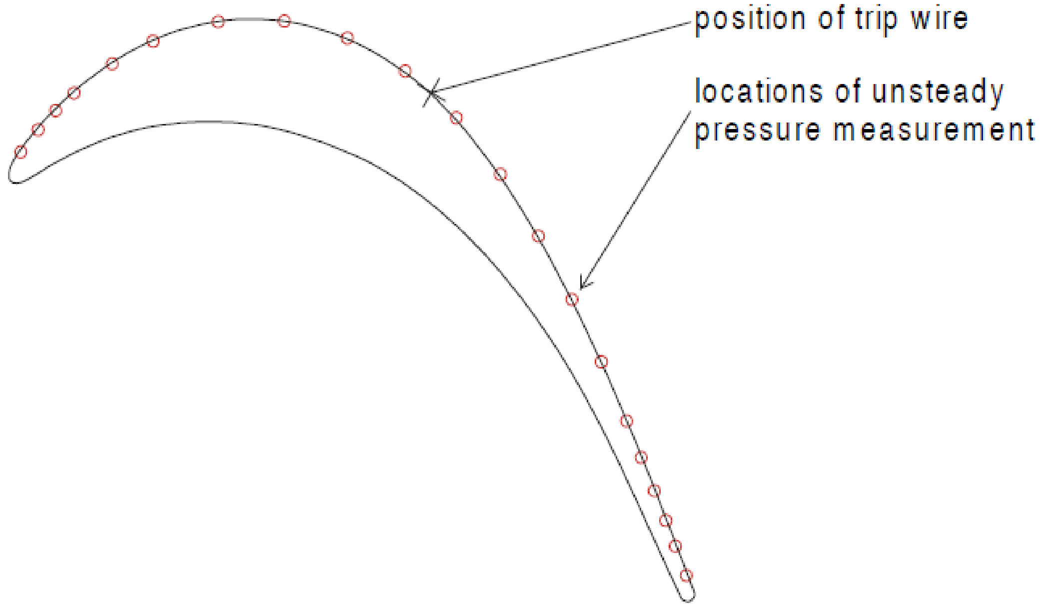

Stieger(2002)

- Most extensively studied LPT blade
- Used in PW2037 engine
- Test results from Universitat der Bundeswehr in Munchen, available as semi-open literature

Governing N-S Equations for Compressible Flow

Continuity:

$$\frac{\partial \rho}{\partial t} + \frac{\partial(\rho u_j)}{\partial x_j} = 0$$

Momentum:

$$\frac{\partial(\rho u_i)}{\partial t} + \frac{\partial(\rho u_i u_j)}{\partial x_j} = -\frac{\partial p}{\partial x_i} + \frac{\partial \tau_{ij}}{\partial x_j}$$

Energy:

$$\frac{\partial(\rho E)}{\partial t} + \frac{\partial(\rho u_j H)}{\partial x_j} = \frac{\partial}{\partial x_j}(u_i \tau_{ij}) - \frac{\partial}{\partial x_j} q_j$$

Equation of state:

$$p = \rho R T$$

Energy $E = \dfrac{p}{\rho(\gamma - 1)} + \dfrac{1}{2}\sum_{i=1}^{3} u_i u_i$ Enthalpy $H = E + \dfrac{p}{\rho}$

Governing N-S Equations for Compressible Flow

Constitutive equations

$$\tau_{ij} = \mu \left[\frac{\partial u_i}{\partial x_j} + \frac{\partial u_j}{\partial x_i} - \frac{2}{3}\delta_{ij}\frac{\partial u_k}{\partial x_k} \right]$$

$$q_i = -\kappa \frac{\partial T}{\partial x_i}$$

Sutherland's law for viscosity, thermal conductivity:

$$\frac{\mu}{\mu_{ref}} = \left(\frac{T}{T_{ref}}\right)^{1.5} \left(\frac{T_{ref} + S_\mu}{T + S_\mu}\right)$$

$$\frac{\kappa}{\kappa_{ref}} = \left(\frac{T}{T_{ref}}\right)^{1.5} \left(\frac{T_{ref} + S_\kappa}{T + S_\kappa}\right)$$

S_μ and S_κ are constants for a given fluid.

DNS Code ANUROOP

Type of equations	Compressible Navier-Stokes
Dimensionality	3D
Discretization methodology	Finite volume
Inviscid flux reconstruction	Second order kinetic energy preserving central difference scheme
Viscous flux reconstruction	Green-Gauss method
Time discretization	Explicit (SSPRK-3)
Element type	Hexahedra, prisms, tetrahedra (Unstructured)
Mesh partitioning	METIS
Computer architecture	CPU, GPU (NVIDIA)

Mesh size required for DNS!

Reynolds number	10^5	2×10^5	5×10^5	10^6
Estimated number of mesh cells	1.28×10^9	5.12×10^9	3.2×10^{10}	1.28×10^{11}

T106A blade simulations: Pressure distribution

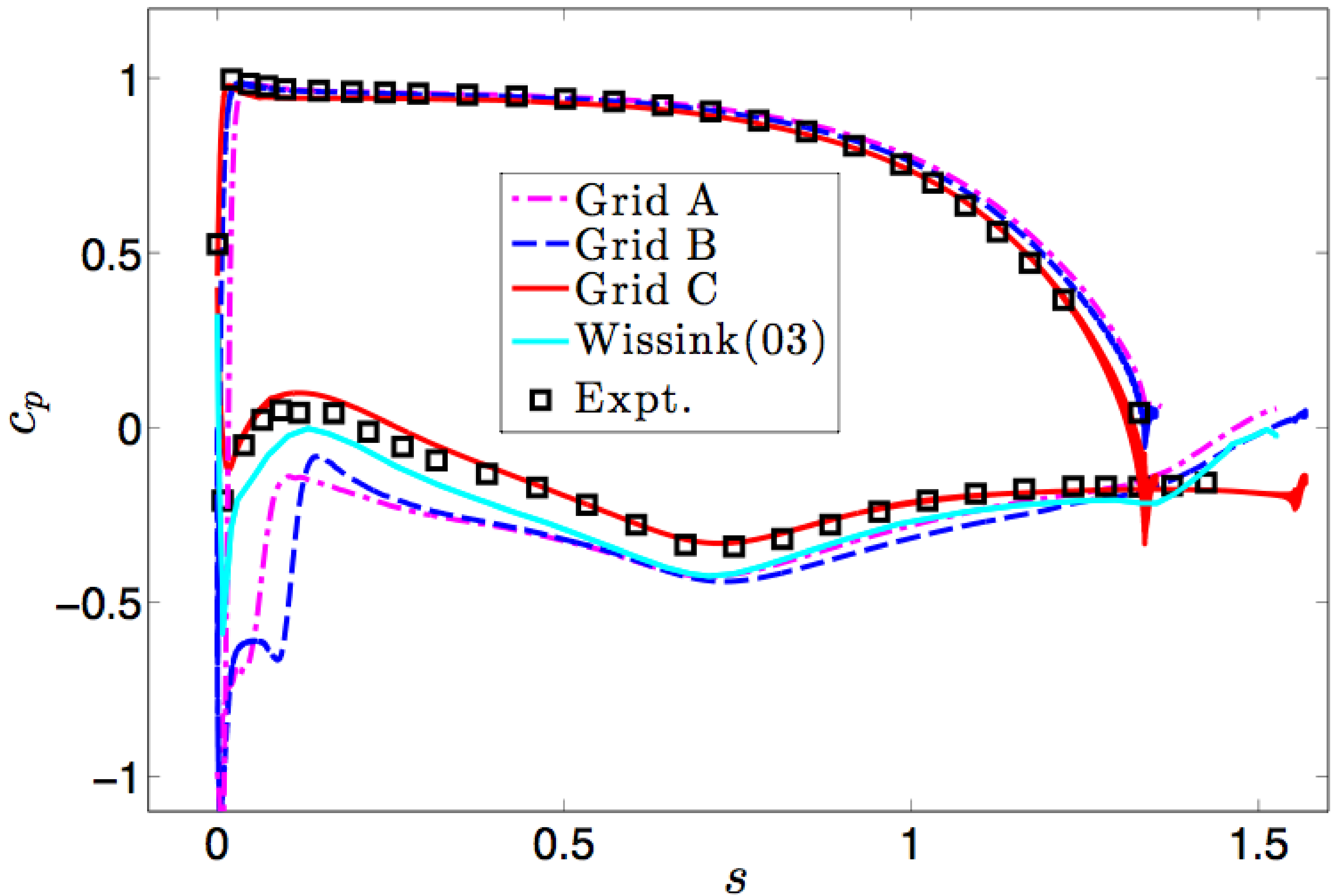

Mean pressure co-efficient along arc length

Pressure side c_p: robust, benign
Suction side c_p: sensitive to resolution

$N \times 10^{-6}$
Wissink (2003): 17; Grid A: 25;
Grid B: 47; Grid C: 161

Separation bubbles

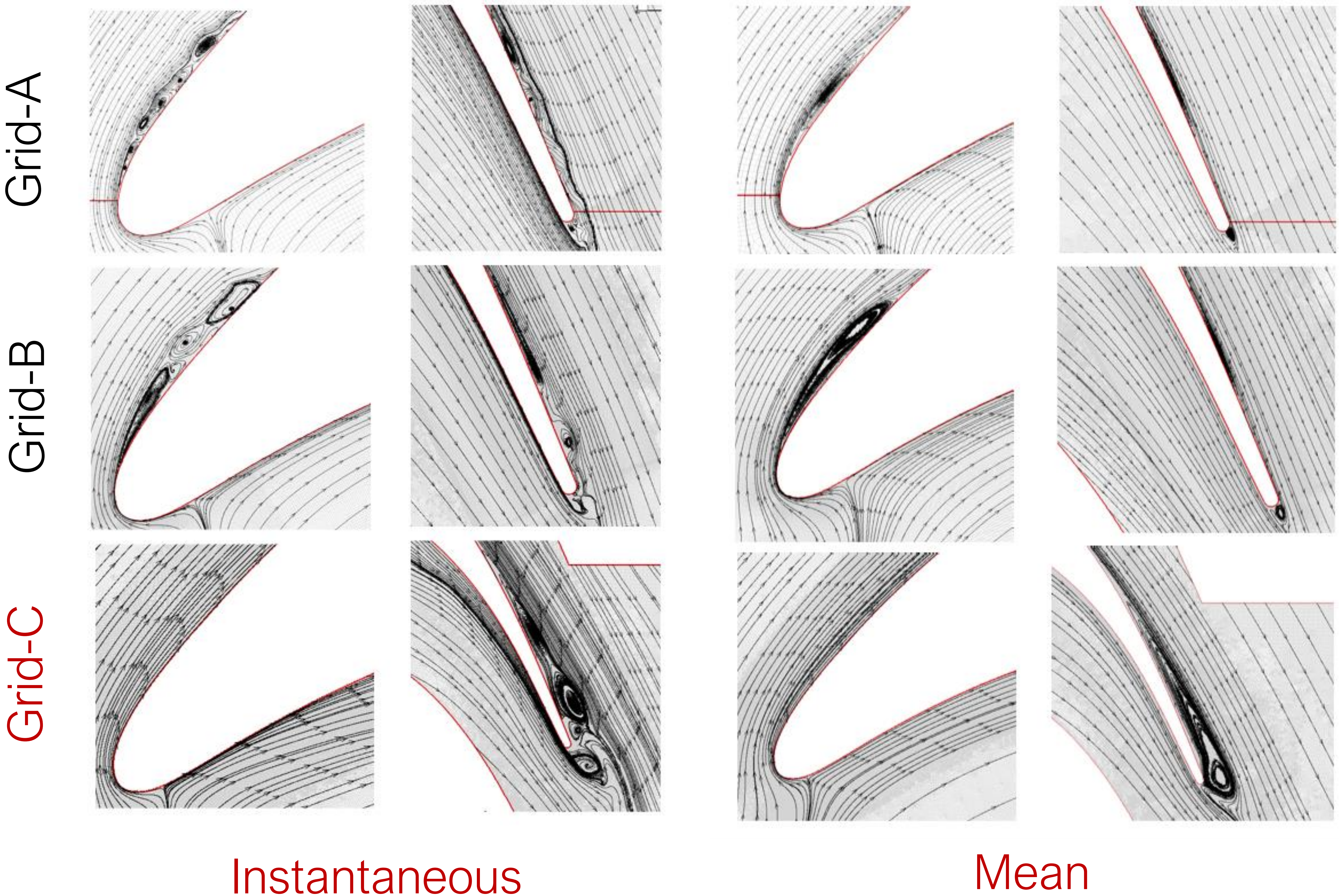

Skin-friction

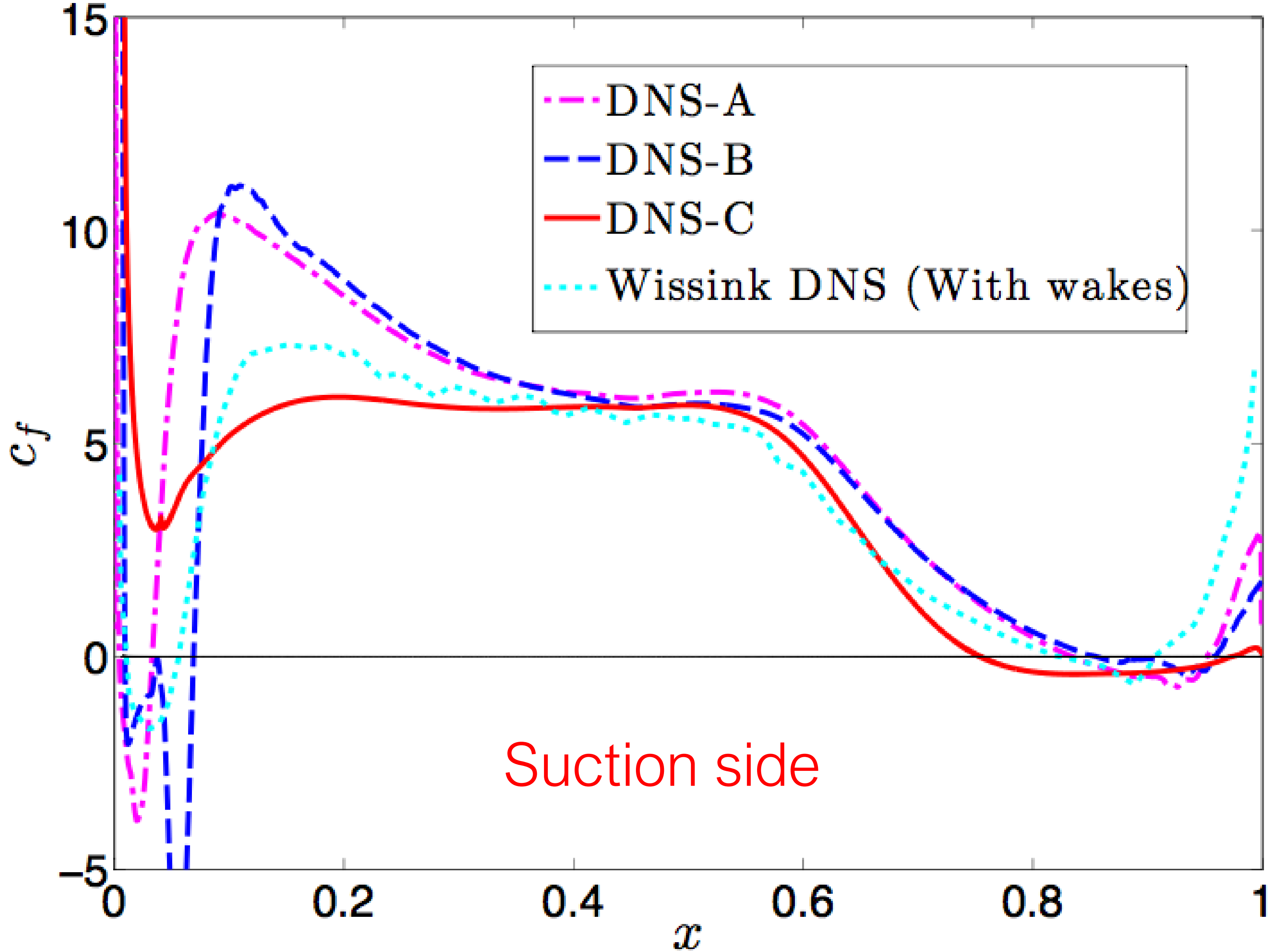

Flow reflects pressure distribution: Strong coupling between C_p and C_f because of transition, relaminarisation…

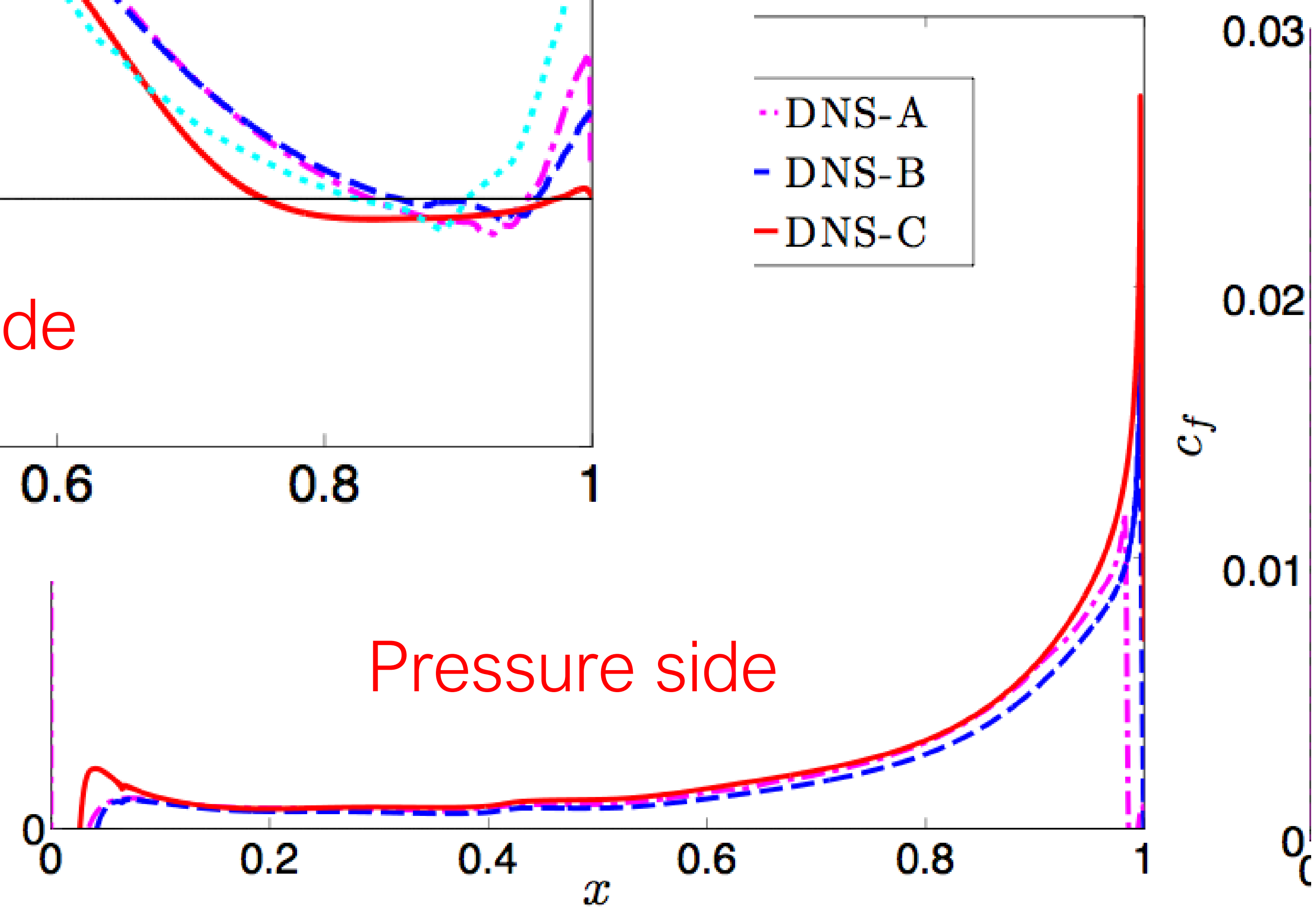

… and separation, and domain of finite size

Curvature effects

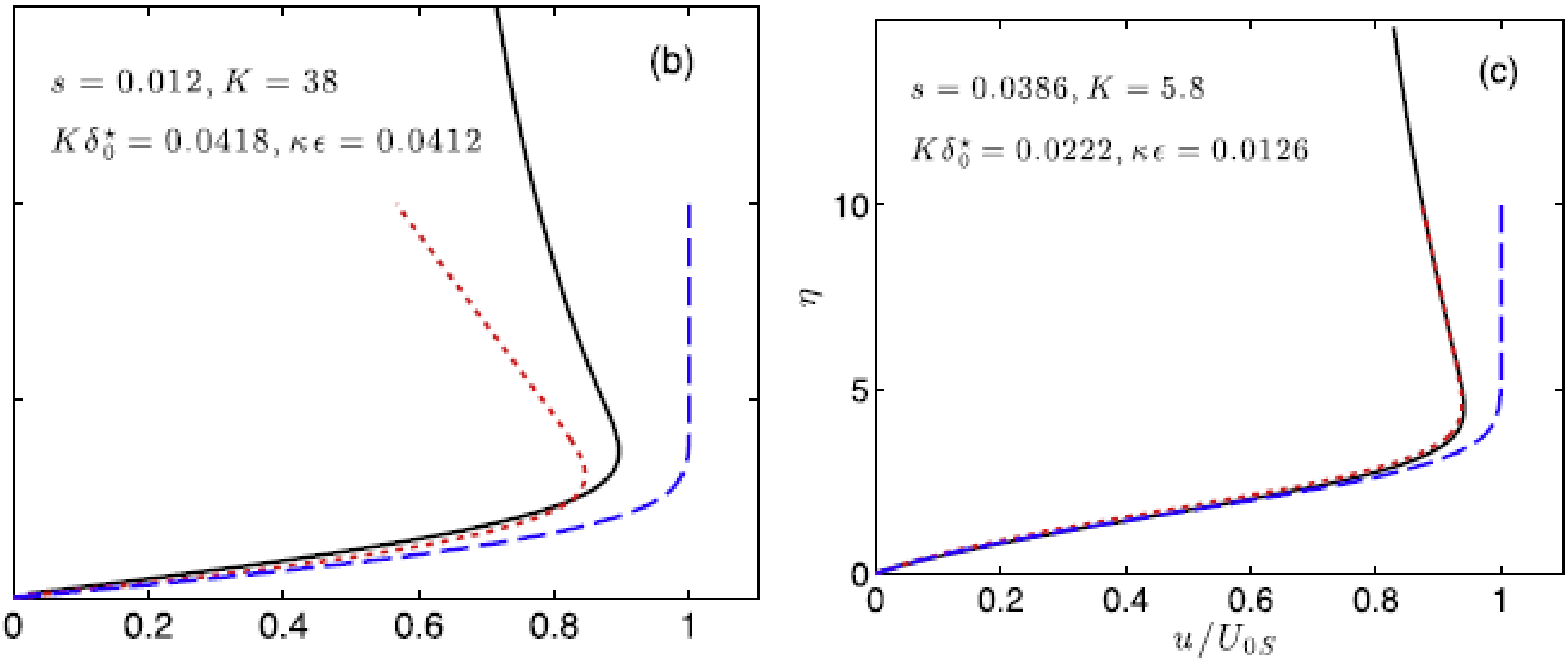

Radius of curvature $R=L_{ax}/K$

$K_{max}=130$

[1]Ranjan++ 2017 Comp. Fluids

Curvature effects on relaminarization

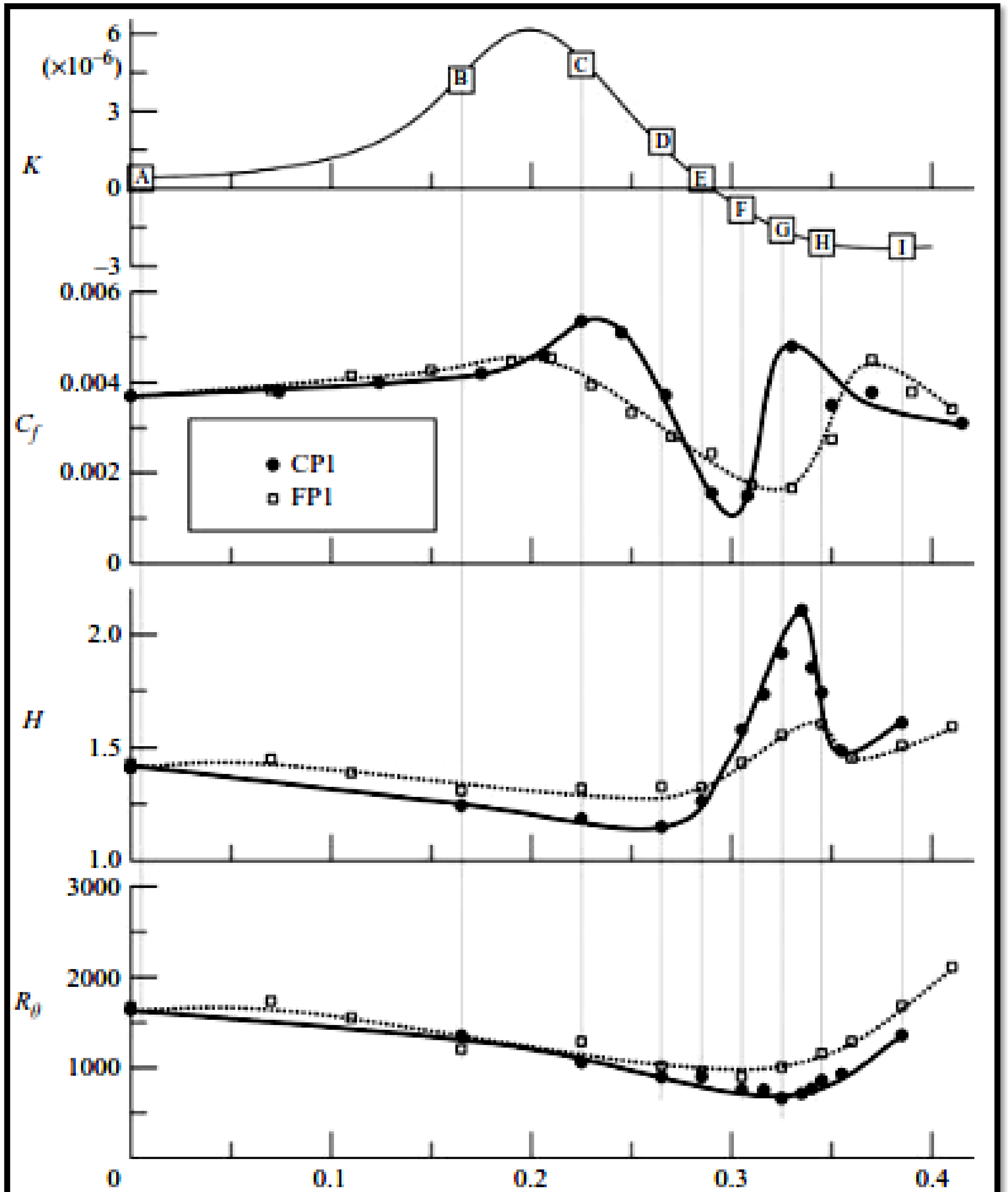

Comparison between flat and convex surface boundary layers, both with exactly the same distribution of the Launder pressure gradient parameter

$$K = \nu(dU_e/dx)/U_e^2$$

(a) CPI=convex surface, FPI=flat Plate. **Letters A,B...I mark hotwire stations. Note sharp, short changes in** c_f and shape factor H. Shows how both transition (rising c_f) and relaminarization **(falling** c_f) are much more rapid and cover much shorter extents streamwise on CPI, compared to FPI.

Mukund et al.2006 JFM

L-T-R-T cycle (Fake)

Grid A

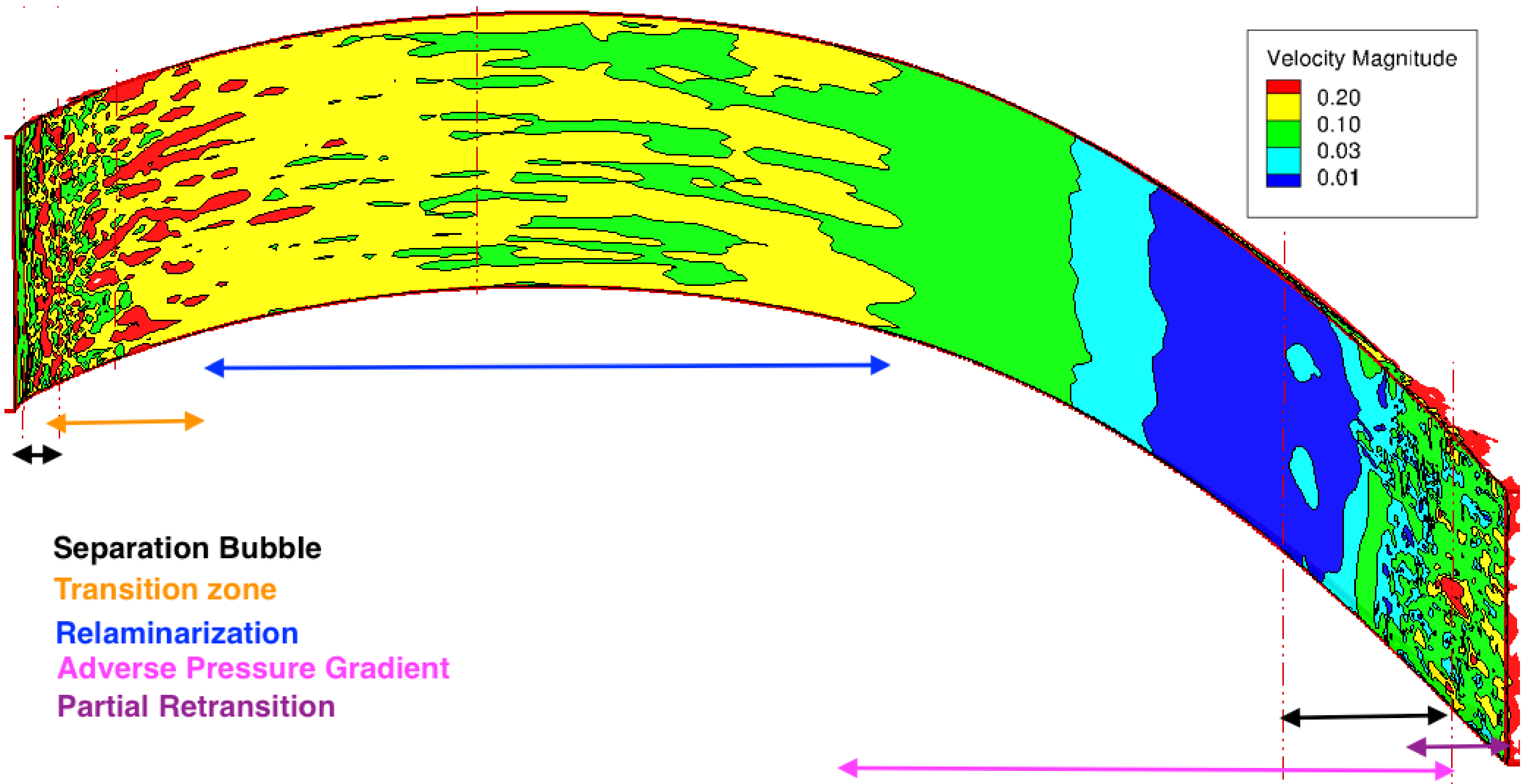

Total velocity contour adjacent to the blade on the suction side

[1]Ranjan et al. (2016) EMU report Aero 2016:1

Scatter plot for C_f (Fake)

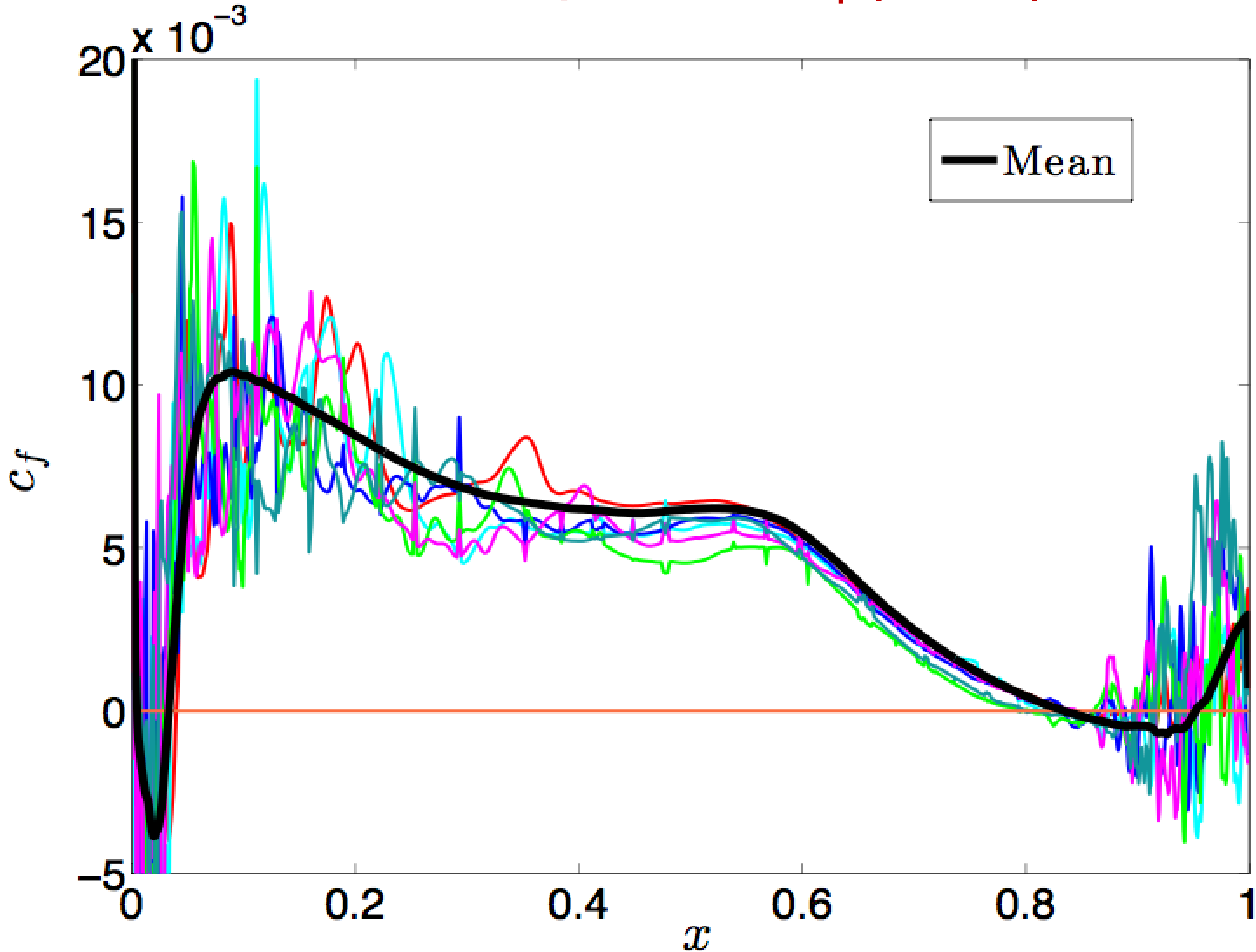

[1]Ranjan et al. (2016) EMU report Aero 2016:1

DNS on STFE blade

ANUROOP-GPU[1]

Scaling of ANUROOP

Weak scaling: Scaling behavior when the work/GPU or CPU (i.e., number of mesh cells per GPU or CPU) is kept constant and number of GPUs or CPUs is increased gradually to solve larger problem

Strong scaling: Scaling behavior when the total grid size is kept constant but number of processors is increased gradually

RDP (Rate of Data Processing): time taken by code per mesh cell per iteration

DHRUVA-3: K20 GPU; IBM Minsky P100; SahasraT, IISc: CPUs

Weak Scaling (on P100 GPU cluster, IBM Minsky

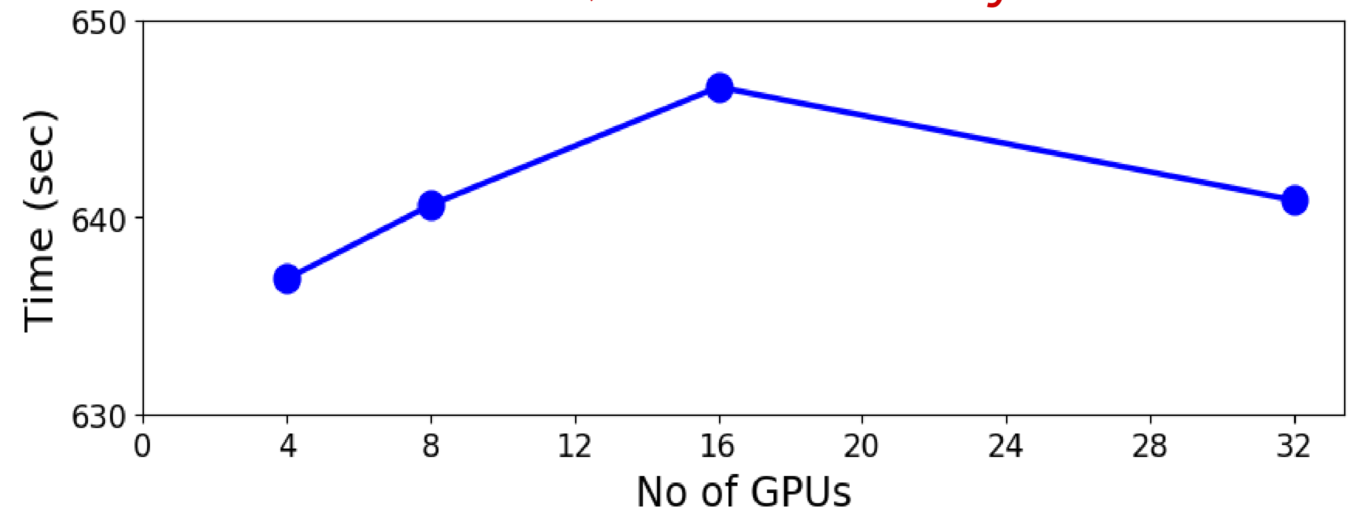

Strong scaling: 240 Million cells, and 1000 iterations

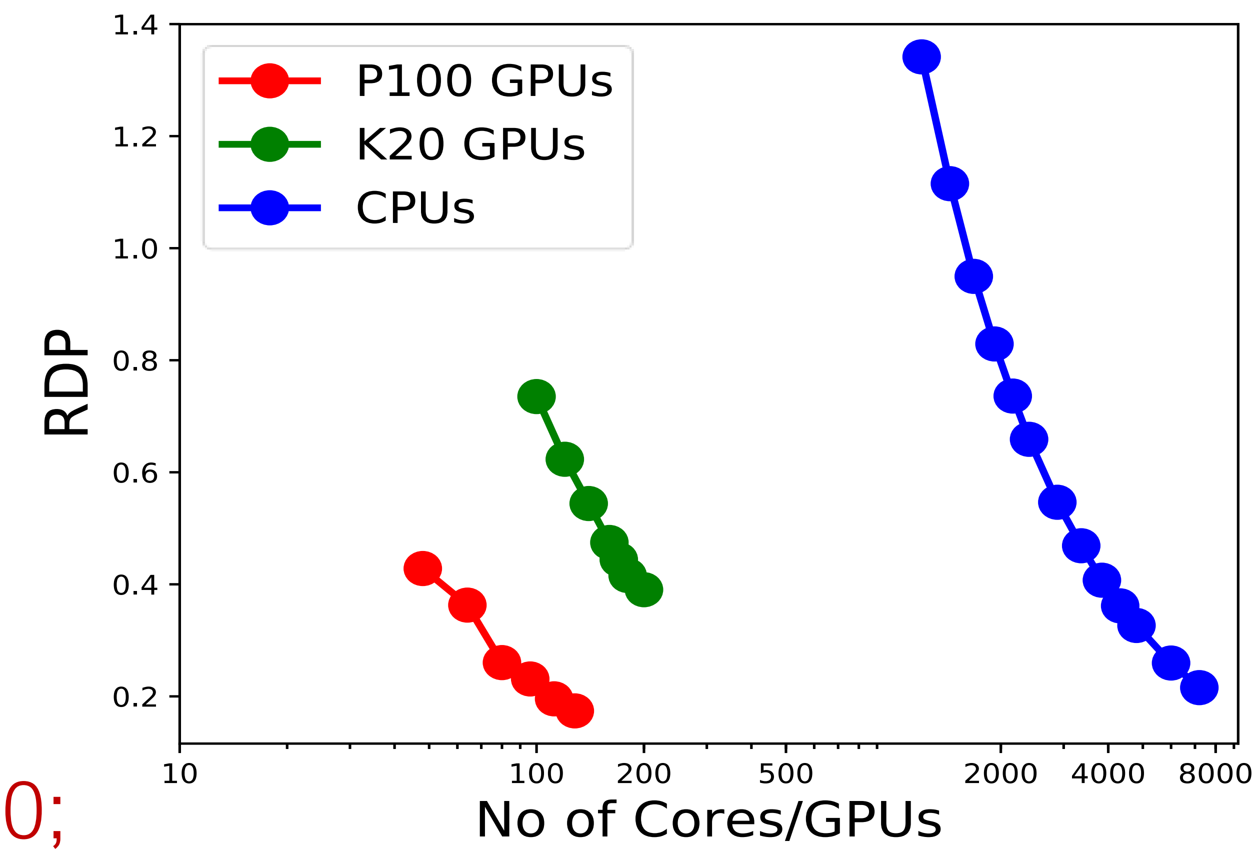

[1]Maruthi et al. (2017)AESI CFD Sym.

Computational Domain for STFE[1]

- 3D stacked mesh
- Flow is 2D in the mean
- Stator blades for STFE
- Compressible NSE
- Unstructured grids
- Boundary layer resolution near wall $Y^+ < 1$
- Used ANUROOP2 for DNS
- Used CFD++, version 16.04, Metacomp Technologies for RANS and LNS

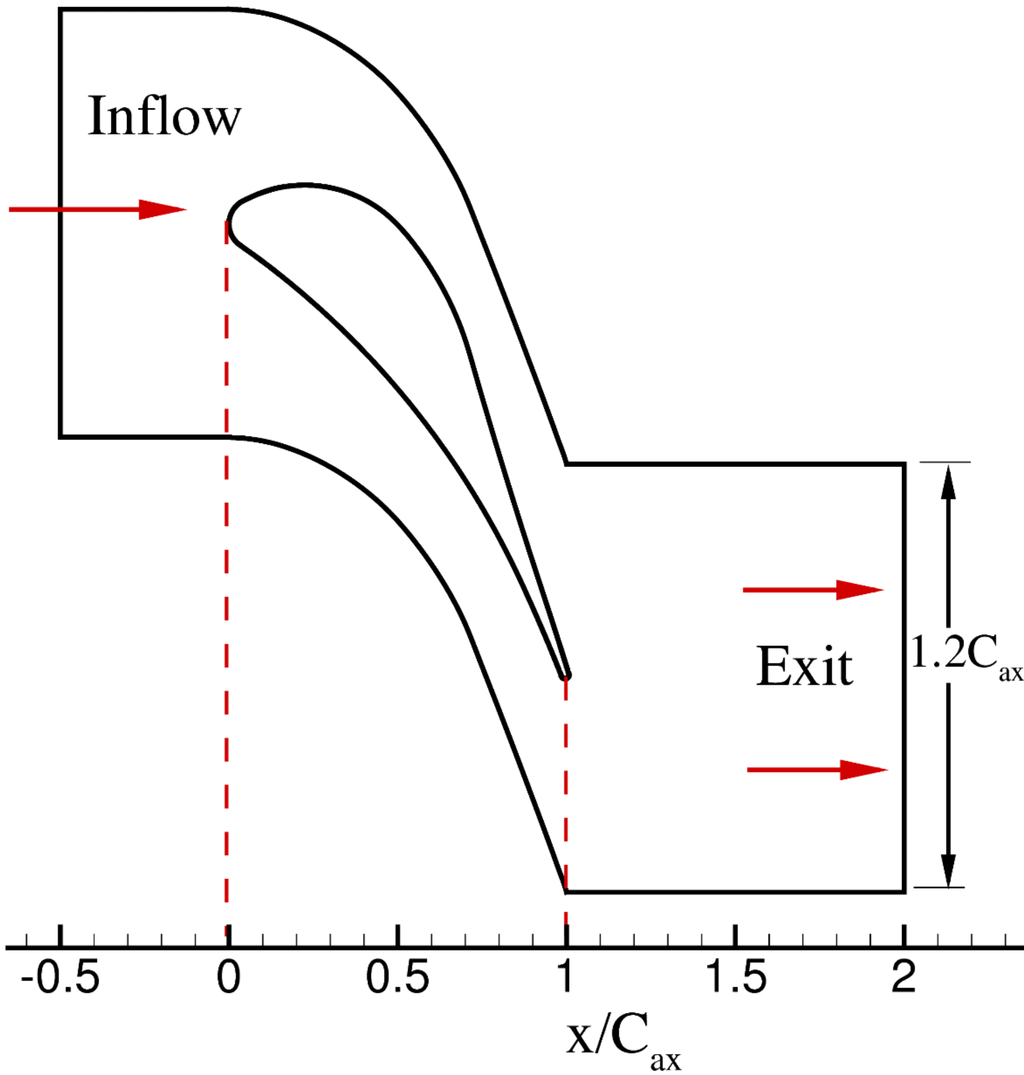

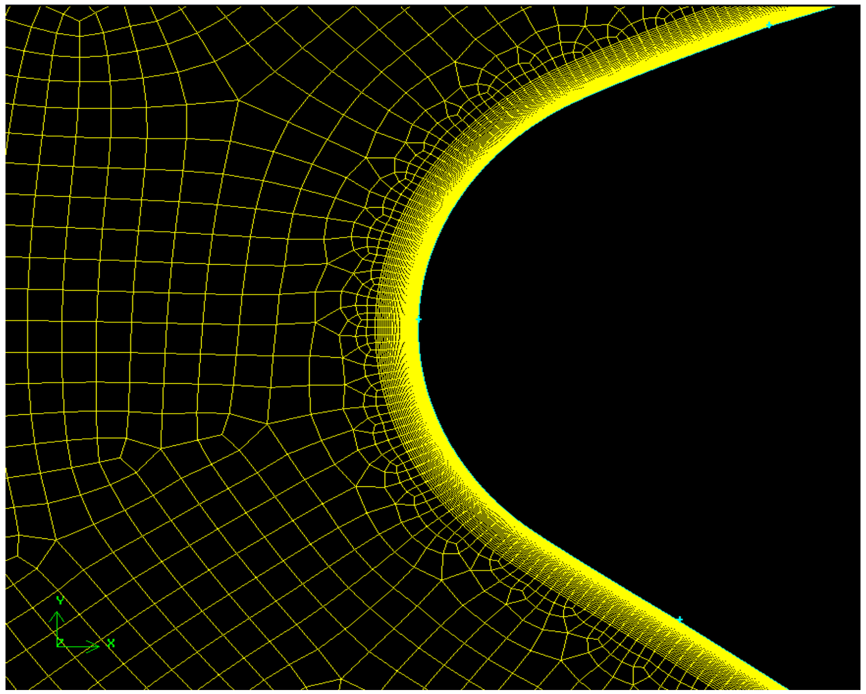

[1]Kishore et al. (2017) AESI CFD Sym.

Grid Details

Simulations	Grid	N_{2D}	N_Z	$N_{total}(\times 10^{-6})$	$\frac{\Delta y_n}{C_{ax}}$ $(\times 10^{5})$	SR	LBG $\frac{y_n}{C_{ax}}(\times 10^{2})$
RANS, LNS	A	161,169	22	3.54	5.86	1.027	1.38
RANS, LNS	B	237,037	43	10.2	5.86	1.027	1.67
DNS	C	733,841	128	93.9	9.02	1.025	1.22

N_{2D}: Total number of elements on 2D face

N_Z: no. of intervals in spanwise direction

$\frac{\Delta y_n}{C_{ax}}$: Height of first cell normal to the blade surface

SR: successive ratio of grid dimensions normal to surface

LBG: last boundary layer grid point

Test case-1: Experimental flow condition[1]

Parameter		Inlet (1)	Exit (2)
Reynolds number	*Re*	152,000	486,000
Mach number	*M*	0.16	0.593
Total pressure (kPa)	P_0	117.750	116.777
Static pressure (kPa)	P	115.657	92.072
Static temperature (K)	*T*	298	-
Flow direction		AoA = 0	72.1 deg. from axis

[1]Kumaran et al. (2014) NAL report

Test case-1: Coefficient of pressure, C_p

$$C_p = \frac{p - p_2}{p_{01} - p_2}$$

- DNS at 93.9×10^6 Mesh cells
- LNS and SST are close to each other, and to both DNS and experimental results, compared to RKE

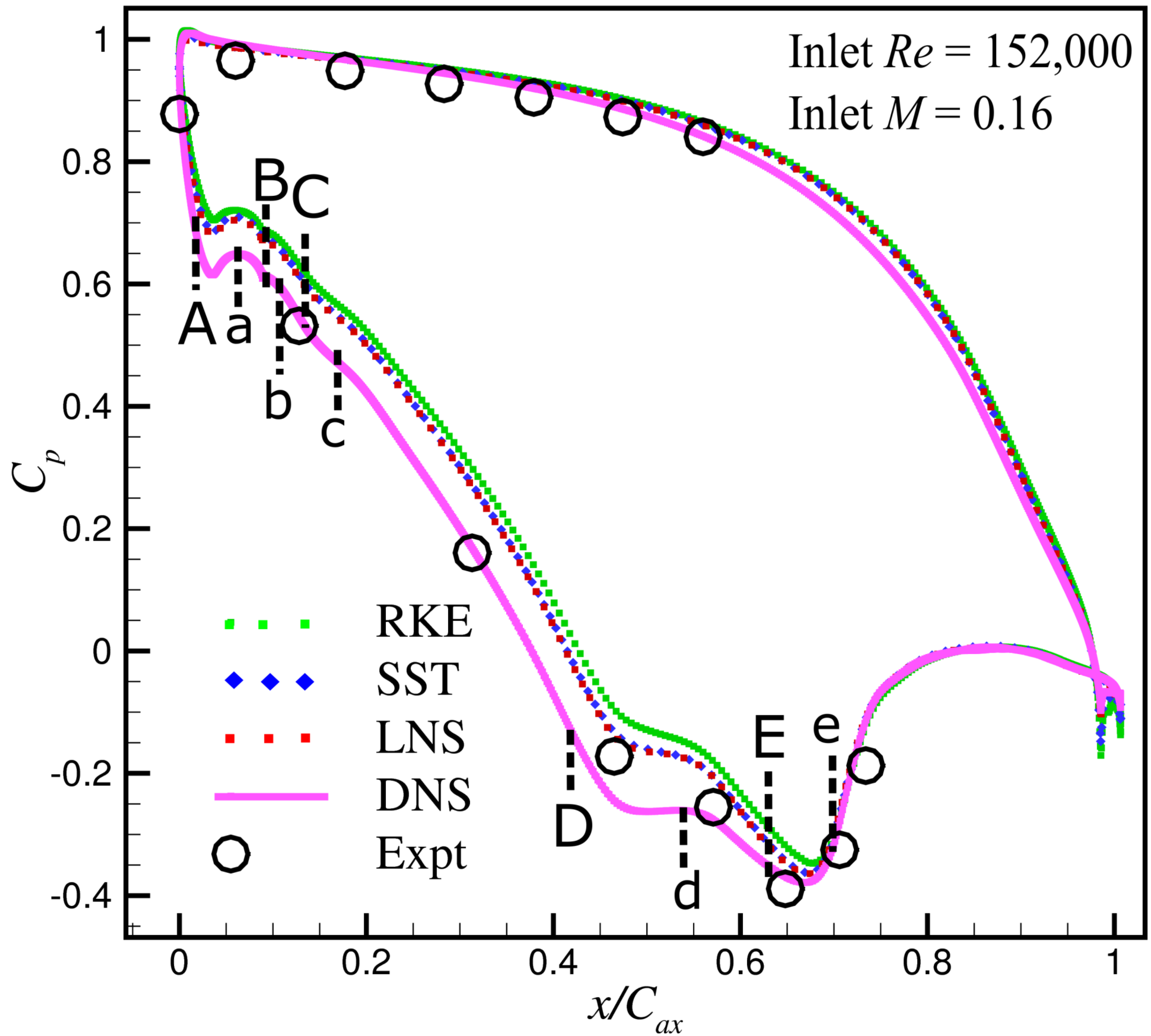

Test case-1: Skin friction coefficient (C_f)

Pressure surface

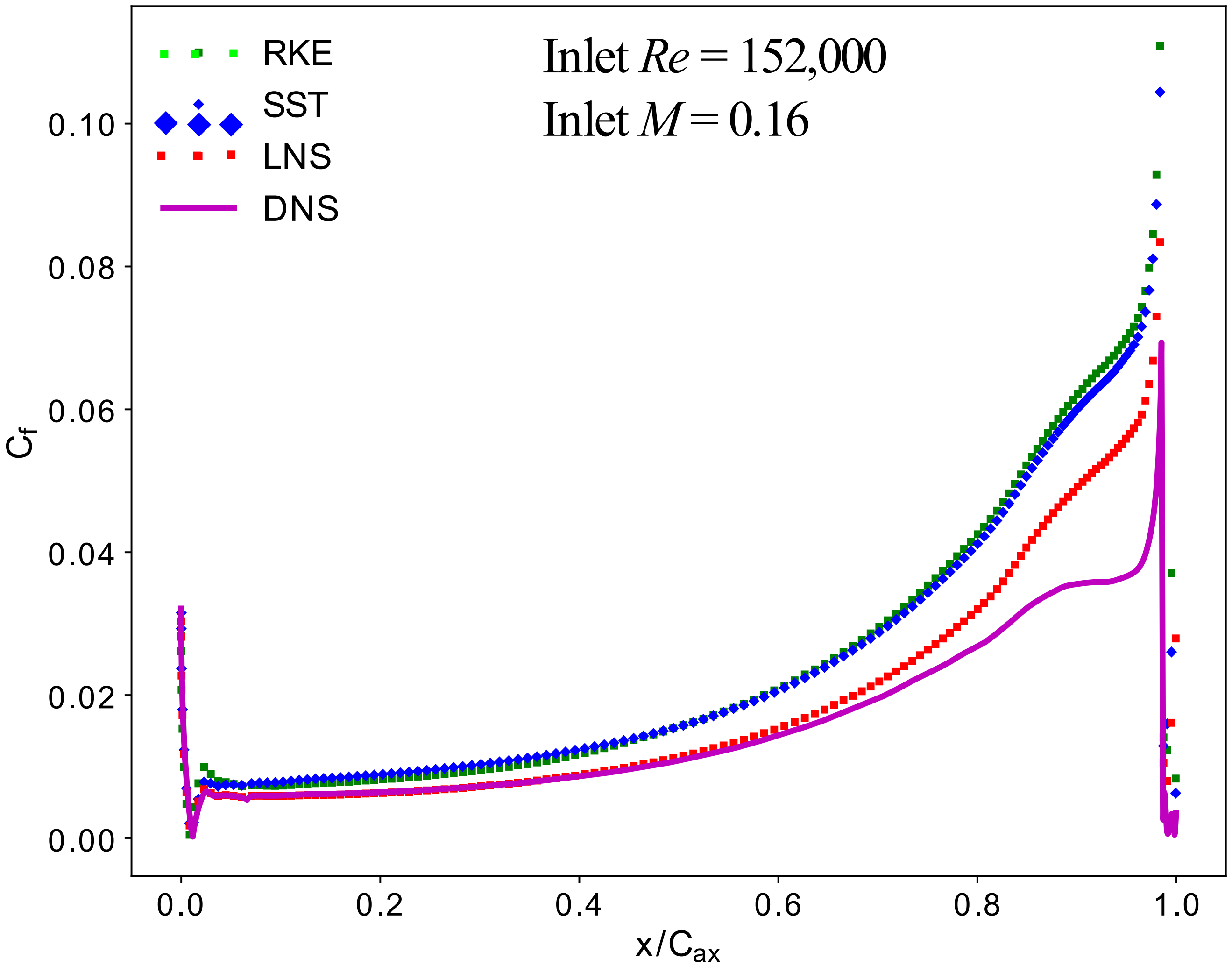

Suction surface

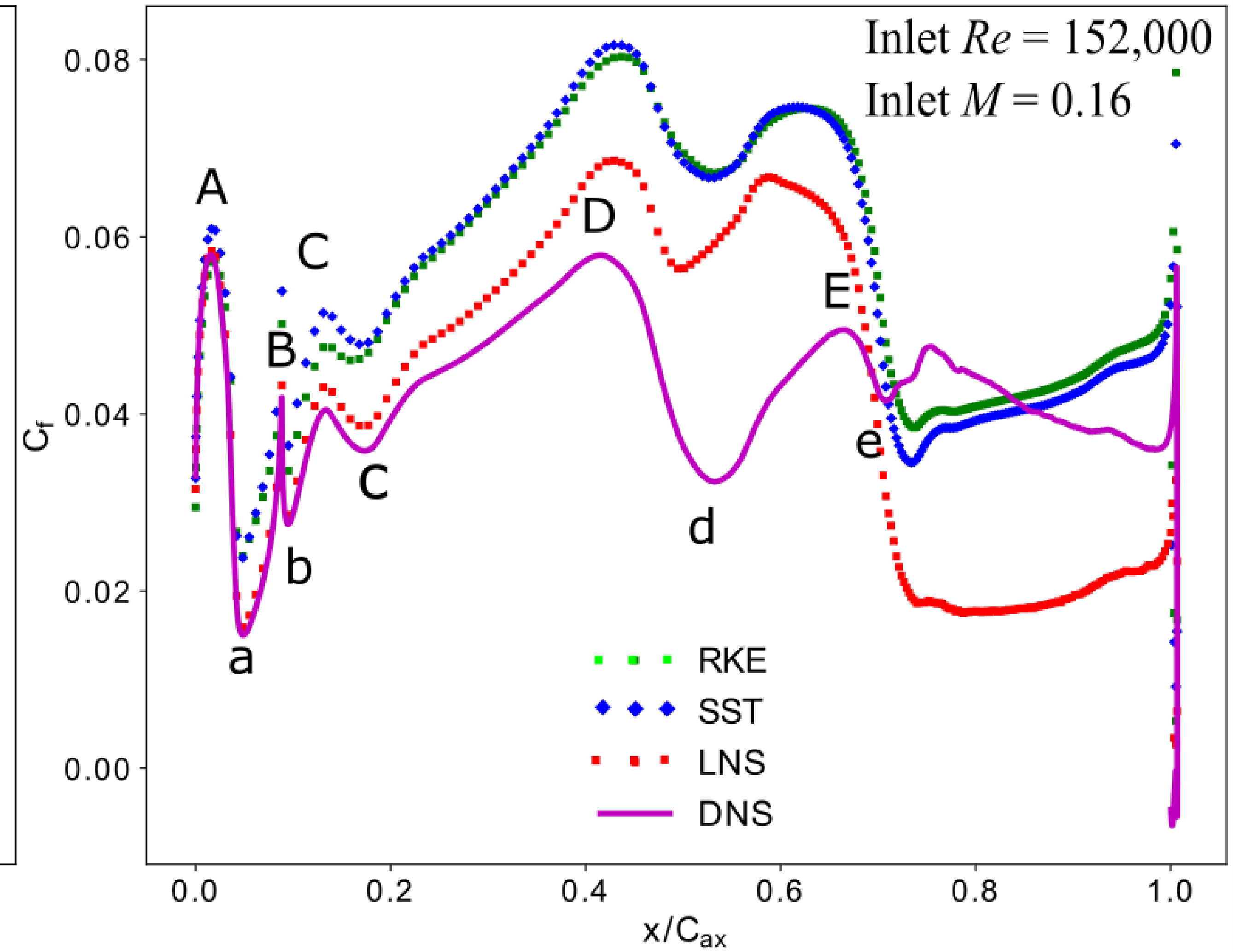

LNS is closest to DNS result for the complete chord length

LNS is closer to but higher than DNS till $0.7C_{ax}$ and lower beyond this point, while the SST is closer beyond $0.7C_{ax}$

PRESSURE DISTRIBUTION WITH HIGHER RESOLUTION

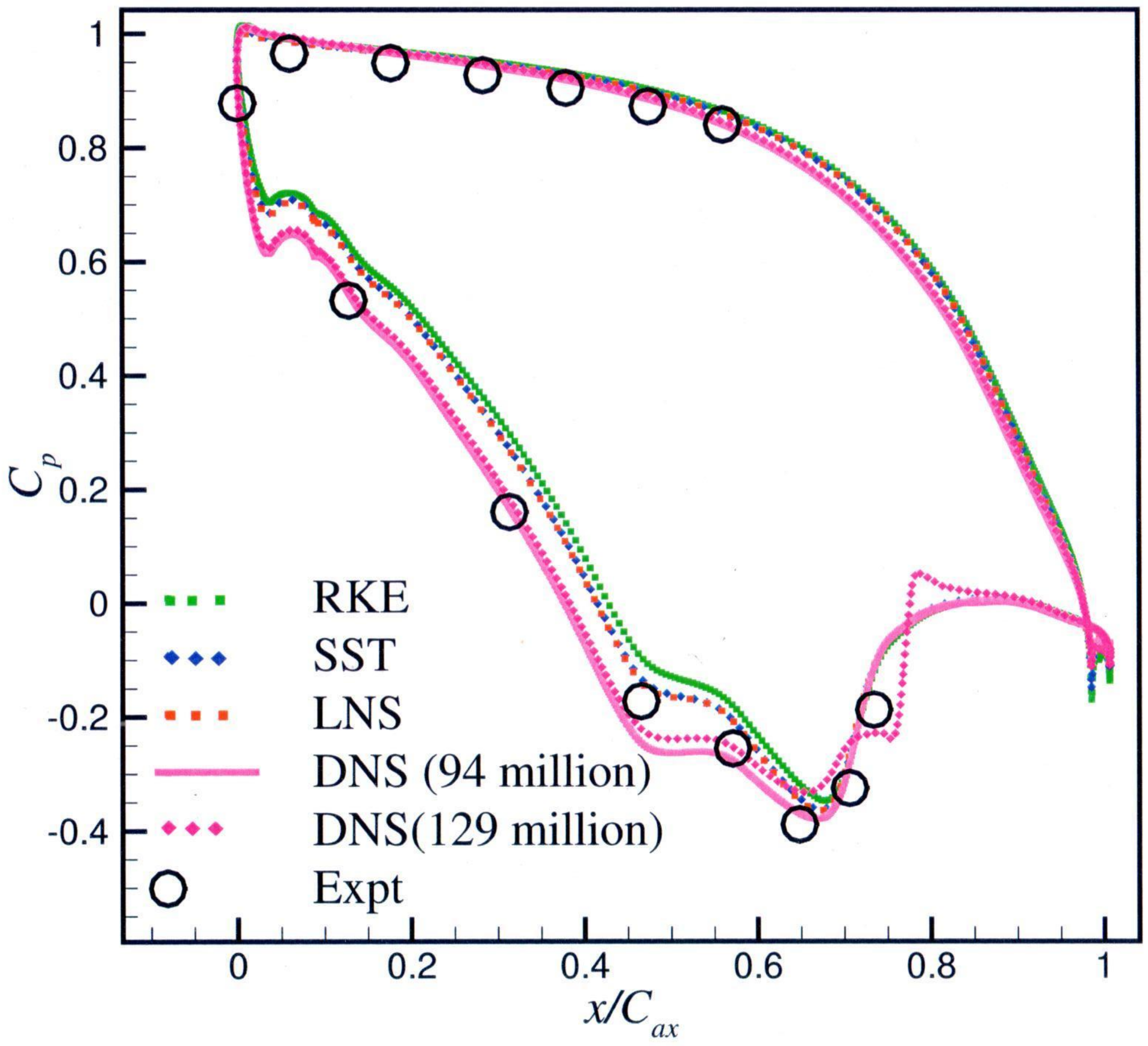

SKIN FRICTION WITH HIGHER RESOLUTION

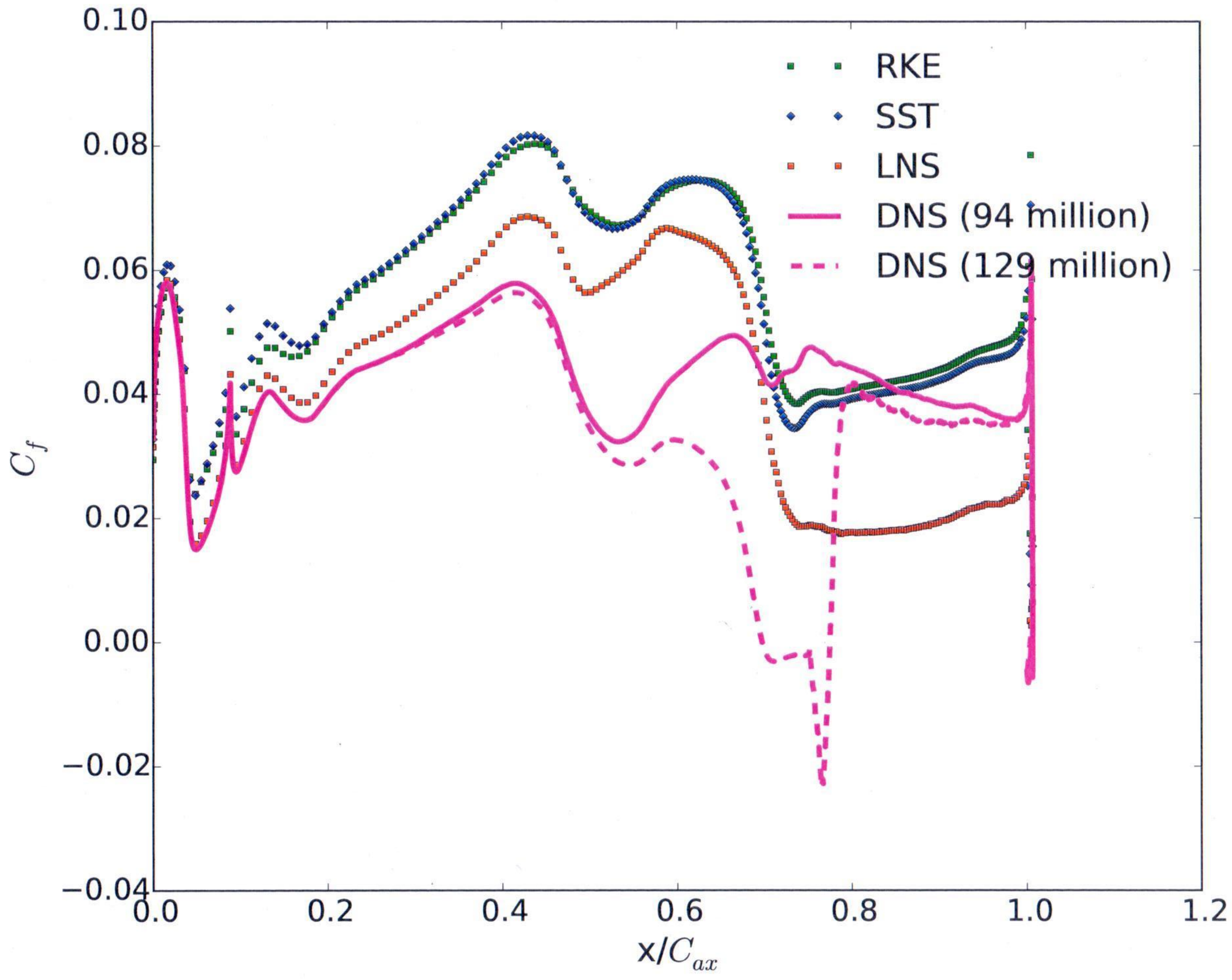

Note separation bubble at x/C_{ax} near 0.8

Test case-2: Turbine operating conditions

Parameter		Inlet (1)	Exit (2)
Reynolds number	*Re*	314,270	692,000
Mach number	*M*	0.29	1.34
Total pressure (kPa)	P_0	762.50	738
Static pressure (kPa)	P	718.50	252
Total temperature (K)	T_0	1317.39	
Static temperature (K)	*T*	1295.2	969.03
Angle of Attack	AoA	0	-

Test case-2: Mach number contours

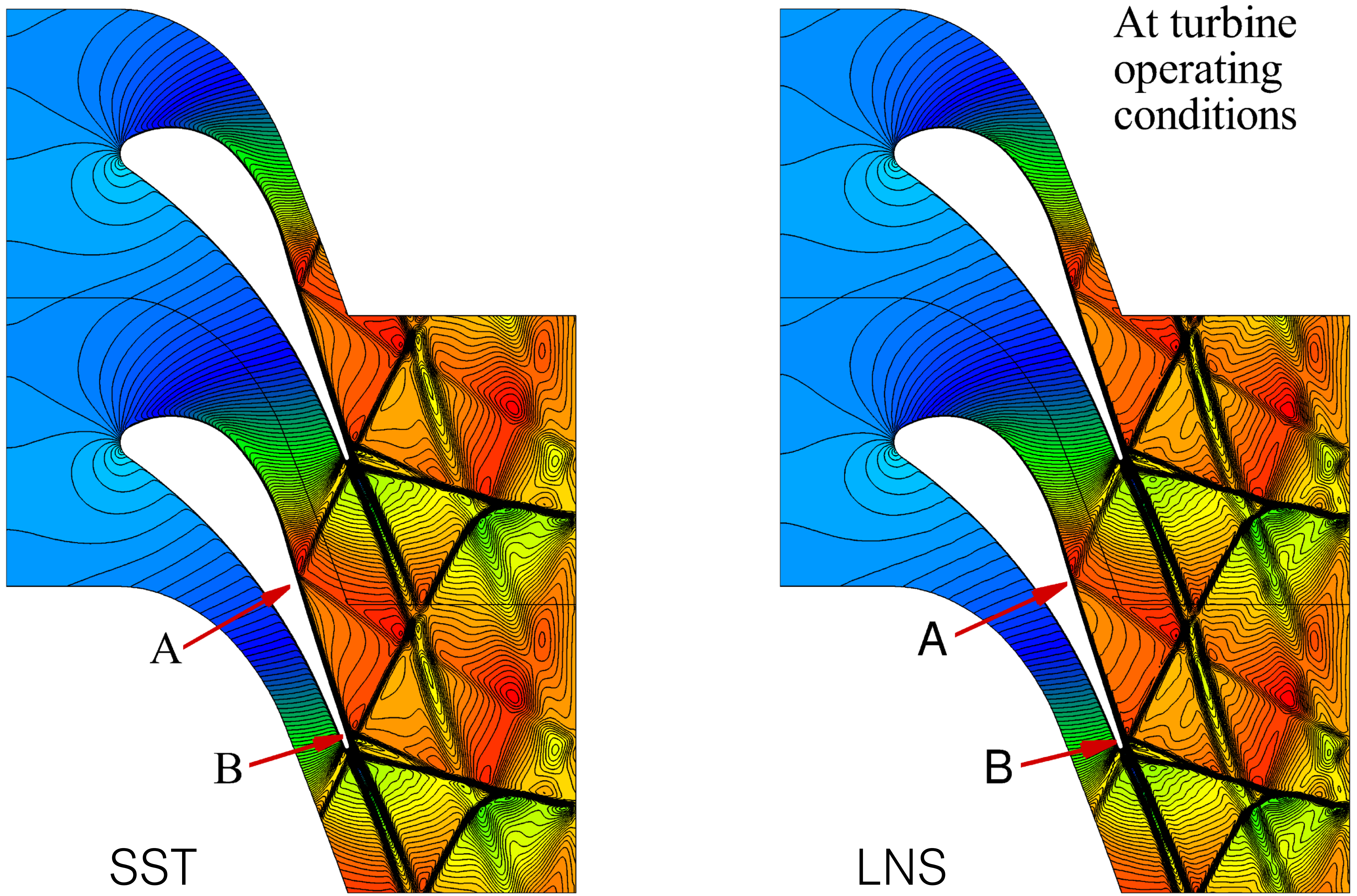

Test case-2: Pressure coefficient (C_p)

- Inlet M_1=0.29 and Re_1=314,000
- Exit M_2=1.34 and Re_2=692,000
- Inlet static temperature = 1295.2K
- Modest difference between LN and SST

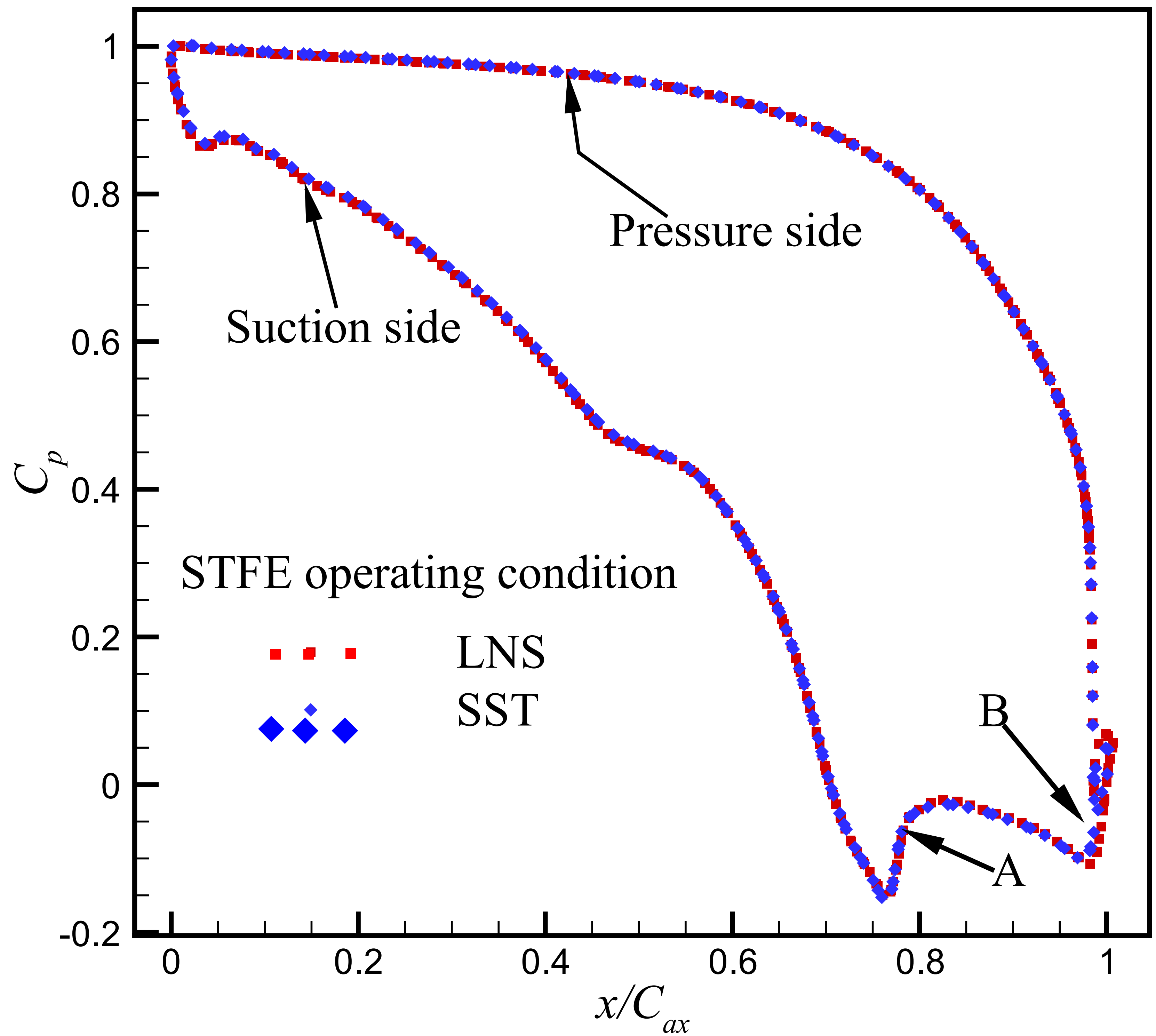

Test case-2: Skin friction coefficient (C_f)

- Inlet M_1=0.29 and Re_1=314,000
- Exit M_2=1.34 and Re_2=692,000
- Inlet static temperature = 1295.2K
- LNS and SST closely agree

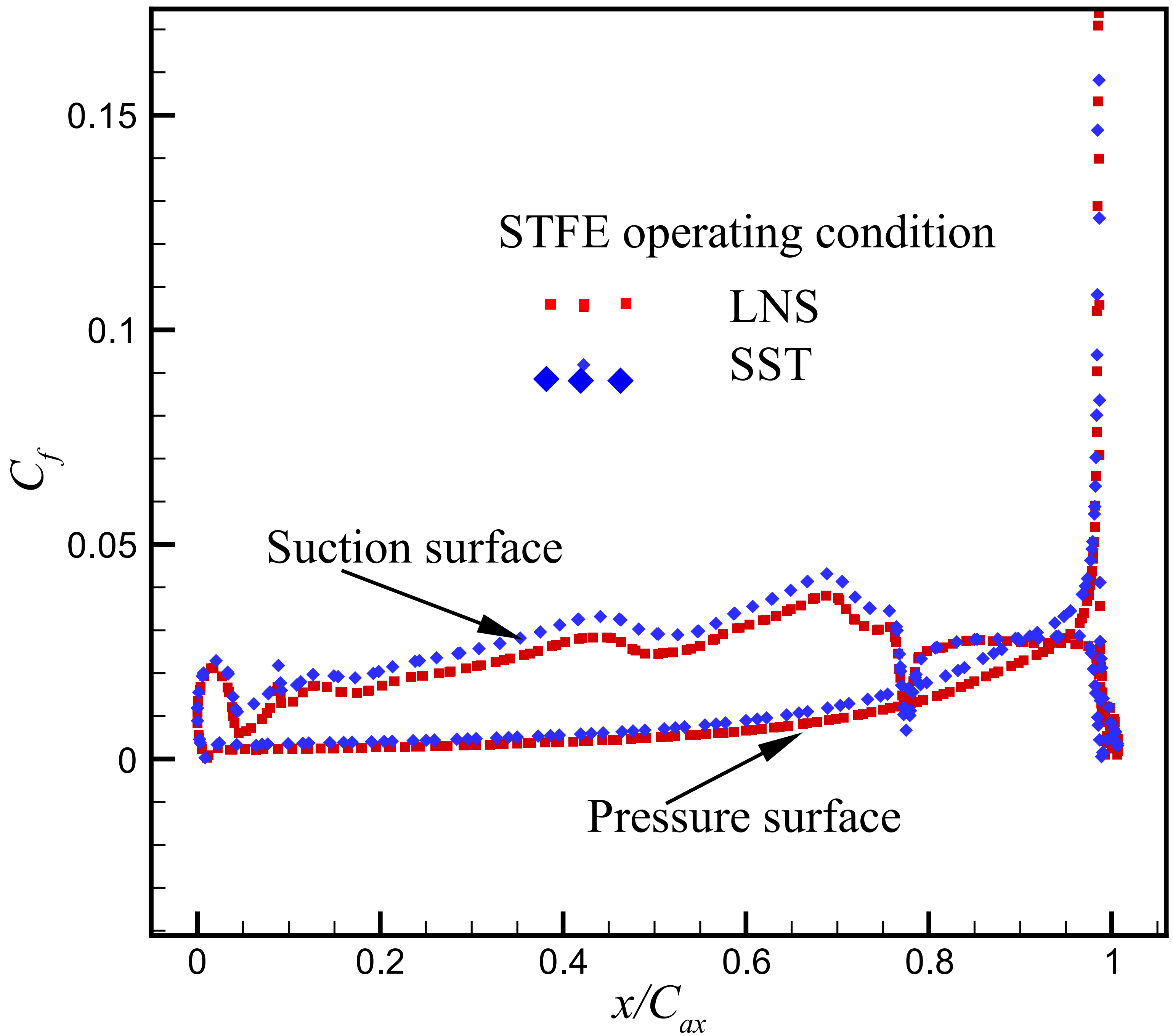

Test case-2: Static temperature distribution (*T*)

- Inlet M_1=0.29 and Re_1=314,000
- Exit M_2=1.34 and Re_2=692,000
- Adiabatic wall
- LNS and SST differ slightly (<5K) along the pressure surface upto appr. 0.8 C_{ax}…
- …while along the suction surface they differ by up to 20K near the trailing edge (x/ C_{ax}>0.8)

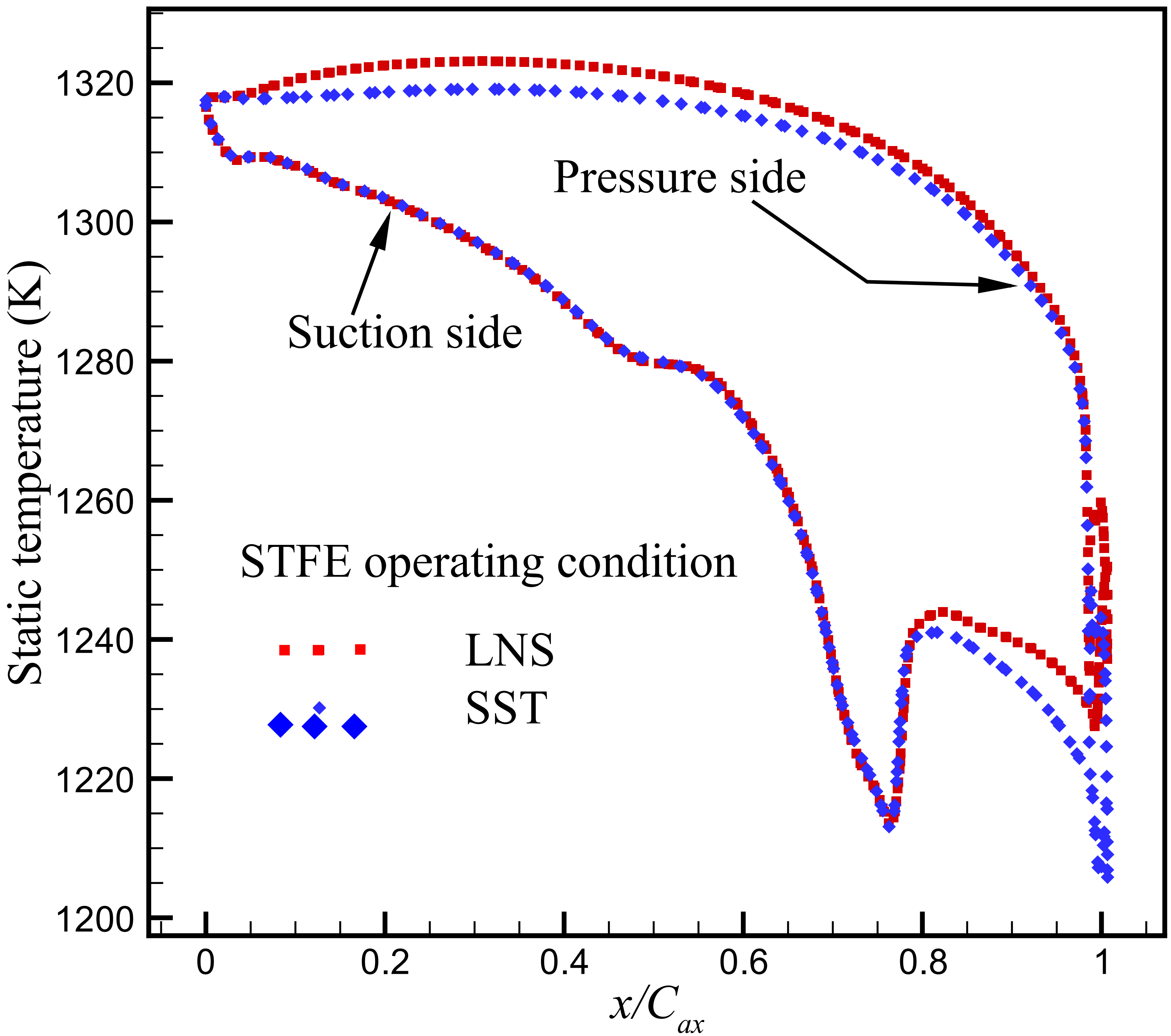

Conclusions

WHY ZOO ON THE TURBINE BLADE?

- Blade Reynolds numbers in "modest" range 10^5-10^6- not low, not high: (cf. instability-critical Re_x on flat plate=$1.12x10^5$). So: vulnerable to rapid changes in pressure.
- Blade curvature sharpens both direct and reverse transition.
- Blade curvature very high near leading edge: not amenable to Prandtl's theory nor even to its first-order correction.
- Suction side beyond RANS, sensitive to resolution, can exhibit dramatic changes. Can be handled by DNS; LNS is second best.
- Pressure side shows smooth behaviour, amenable to RANS, LNS models
- DNS results with adequate resolution agree with experiments

Conclusions

- Strong coupling between C_p and C_f, and flow events like transition, relaminarisation and separation in the “modest” Re-range. Effects stronger in confined domain
- LNS does not always agree with DNS, but is generally closer to DNS than any other model (including LES)
- For STFE operating conditions at inlet *Re*=314,270 and inlet *M*=0.29, SST and LNS promise results closest to the DNS solution for C_p, C_f and shock boundary layer interactions
- Based on experience with ANUROOP (on several GPU clusters), recommend use of GPU-based heterogeneous supercomputers for HPC in CFD. They can provide results for bigger problems (e.g. at higher ***Re***) in more realistic time frames. Simulation of flow past gas turbine blades at more practical ***Re*** seems to be getting closer to reality

Acknowledgements

Work reported here supported by three research grants (two by GTRE and one by ANURAG)

Thank you

TWO GREAT EXAMPLES OF ROSHKO'S WORK

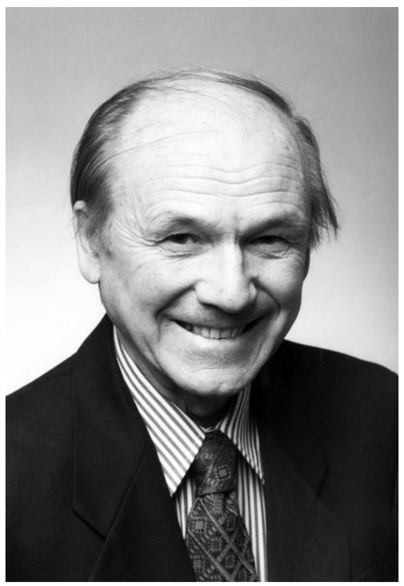

-

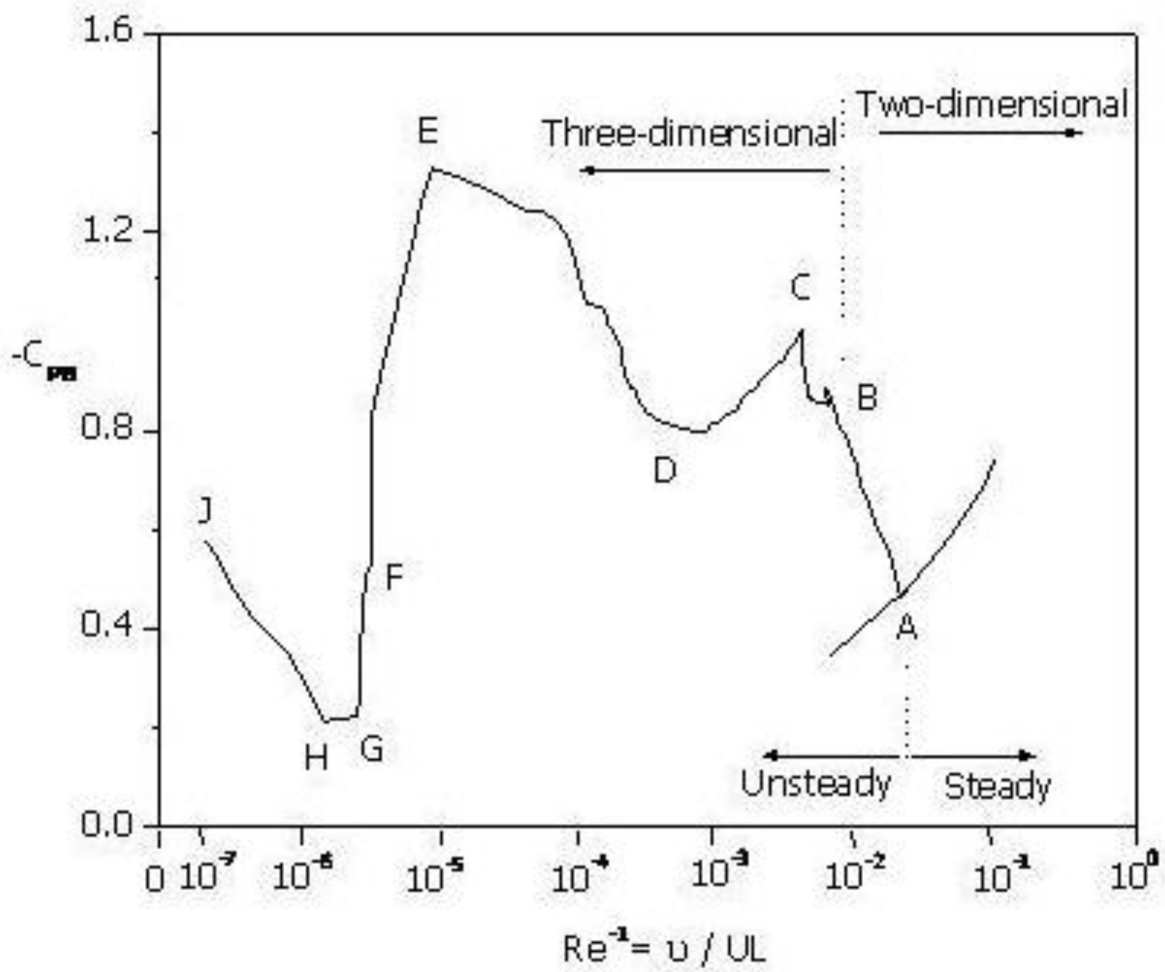

Wake behind circular cylinder : crazy route to zero viscosity

Roshko (1993); plotted on quasi-log scale vs Re^{-1}, RN 2008

Coherent structures in a fully turbulent mixing layer: order and disorder

Brown and Roshko 1974 *JFM*